# *LWDM. Warm Dark Matter Galaxies in Agreement with Observations.*

**Norma G. SANCHEZ**

**DR CNRS LERMA Observatoire de Paris**

**Chalonge Meudon Workshop 2013**

**Meudon CIAS 5-7 JUNE 2013**

# CONTENT OF THE UNIVERSE

**ATOMS, the building blocks of stars and planets: represent only the 4 %**

**DARK MATTER comprises 26 % of the universe. This matter, different from atoms, does not emit or absorb light. It has only been detected indirectly by its gravity.**

**70% of the Universe, is composed of DARK ENERGY that acts as a sort of an anti-gravity. This energy, distinct from dark matter, is responsible for the present-day acceleration of the universal expansion, compatible with cosmological constant**

# Basement- ground Zero

**Dark matter is the dominant component of Galaxies and is an essential ingredient to understand Galaxy properties and Galaxy formation**

**Dark matter and Galaxy Formation must be treated in an cosmological context**

**The nature (the type) of Dark Matter and the cosmological model need to be explicitated when discussing galaxies and galaxy formation**

**All the building of galaxy formation depends on**

**the nature of Dark Matter**

# CONTENTS

**(I) The Standard Model of the Universe Includes Inflation**

**(II) THE NATURE OF DARK MATTER IN GALAXIES from Theory and Observations: Warm (keV scale) DM**

**(III) NEW: THE ESSENTIAL ROLE OF QUANTUM PHYSICS IN WDM GALAXIES:**
**Semiclassical framework: Analytical Results and Numerical (including analytical) Results**
**Observed Galaxy cores and structures from Fermionic WDM and more results.**

**(IV) NEW: The generic Galaxy types and properties from a same physical framework: From quantum (compact, dwarfs) to classical (dilute, large) galaxies. Equation of state**

# HIGHLIGHTS

**(I)The Effective (Ginsburg-Landau) Theory of Inflation**

## PREDICTIONS :

**The Primordial Cosmic Banana: non-zero amount of primordial gravitons. And Forecasts for CMB exps.**

**(II) : TURNING POINT IN THE DARK MATTER PROBLEM: DARK MATTER IN GALAXIES from Theory and Observations: Warm (keV scale) dark matter**

## Physical Clarification and Simplification

**GALAXY FORMATION AND EVOLUTION IN AGREEMENT WITH OBSERVATIONS**

**naturally re-insert in COSMOLOGY (LWDM)**

**Analytical Results and Numerical**

# NEW RESULTS

## FERMIONIC QUANTUM WDM and GRAVITATION DETERMINE THE OBSERVED PHYSICAL GALAXY PROPERTIES

**-> Dark matter (DM) is the main component of galaxies. Quantum mechanics is a cornerstone of physics from microscopic to macroscopic systems as quantum liquids He^3, white dwarf stars and neutron stars.**

**-> Recent study : Destri, de Vega, Sanchez, (New Astronomy 22, 39, 2013) suggest that quantum mechanics is also responsible of galaxy structures at the kpc scales and below: near the galaxy center, below 10 - 100 pc, the DM quantum effects are important for warm DM (WDM), that is for DM particles with masses in the keV scale.**

**-> A new approach to galaxy structure with results in remarkable agreement with observations:**

(i) Dwarf galaxies turn to be quantum macroscopic objects for WDM supported against gravity by the WDM fermion pressure

(ii) Theoretical analytic framework based on Thomas-Fermi approach determine galaxy structure from the most compact dwarf galaxies to the largest dilute galaxies (spirals, ellipticals).

The obtained galaxy mass, halo radius, phase-space density, velocity dispersion, are fully consistent with observations.

(iii) Interestingly enough, a minimal galaxy mass and minimal velocity dispersion are found for DM dominated objects, which in turn imply an universal minimal mass m_min = 1.9 keV for the WDM particle.

## - OBSERVED GALAXY CORES vs CDM CUSPS and WDM CORES-

- **Astronomical observations show that the DM galaxy density profiles are cored, that is, profiles which are flat at the center.**

**On the contrary, N-body CDM simulations exhibit cusped density profiles, with a typical 1/r cusped behaviour near the galaxy center**

**r = 0.**

**Classical N-body WDM simulations exhibit cores but with sizes much smaller than the observed cores.**

**We have recently developped a new approach to this problem thanks to Quantum Mechanics.**

- **Fermions always provide a non vanishing pressure of quantum nature due to the combined action of the Pauli exclusion principle and Heisenberg uncertainty principle.**

- **Quantum effects for WDM fermions <u>rule out</u> the presence of galaxy cusps for WDM and <u>enlarge</u> the classical core sizes because their <u>repulsive and non-local</u> nature extend well beyond the small pc scales.**

- **Smoothing the density profile at the central regions has an effect on the whole galaxy halo.**

## ndard Cosmological Model: DM + $\Lambda$ + Baryons + Radiat

- Begins by the inflationary era. Slow-Roll inflation explains horizon and flatness.
- Gravity is described by Einstein's General Relativity.
- Particle Physics described by the Standard Model of Particle Physics: $SU(3) \otimes SU(2) \otimes U(1) =$ qcd+electroweak model.
- Dark matter is non-relativistic during the matter dominated era where structure formation happens. DM is outside the SM of particle physics.
- Dark energy described by the cosmological constant $\Lambda$.

# Standard Cosmological Model: $\Lambda$CDM $\Rightarrow$ $\Lambda$WDM

Dark Matter + $\Lambda$ + Baryons + Radiation
begins by the Inflationary Era. Explains the Observations:

- Seven years WMAP data and further CMB data
- Light Elements Abundances
- Large Scale Structures (LSS) Observations. BAO.
- Acceleration of the Universe expansion: Supernova Luminosity/Distance and Radio Galaxies.
- Gravitational Lensing Observations
- Lyman $\alpha$ Forest Observations
- Hubble Constant and Age of the Universe Measurements
- Properties of Clusters of Galaxies
- Galaxy structure explained by WDM

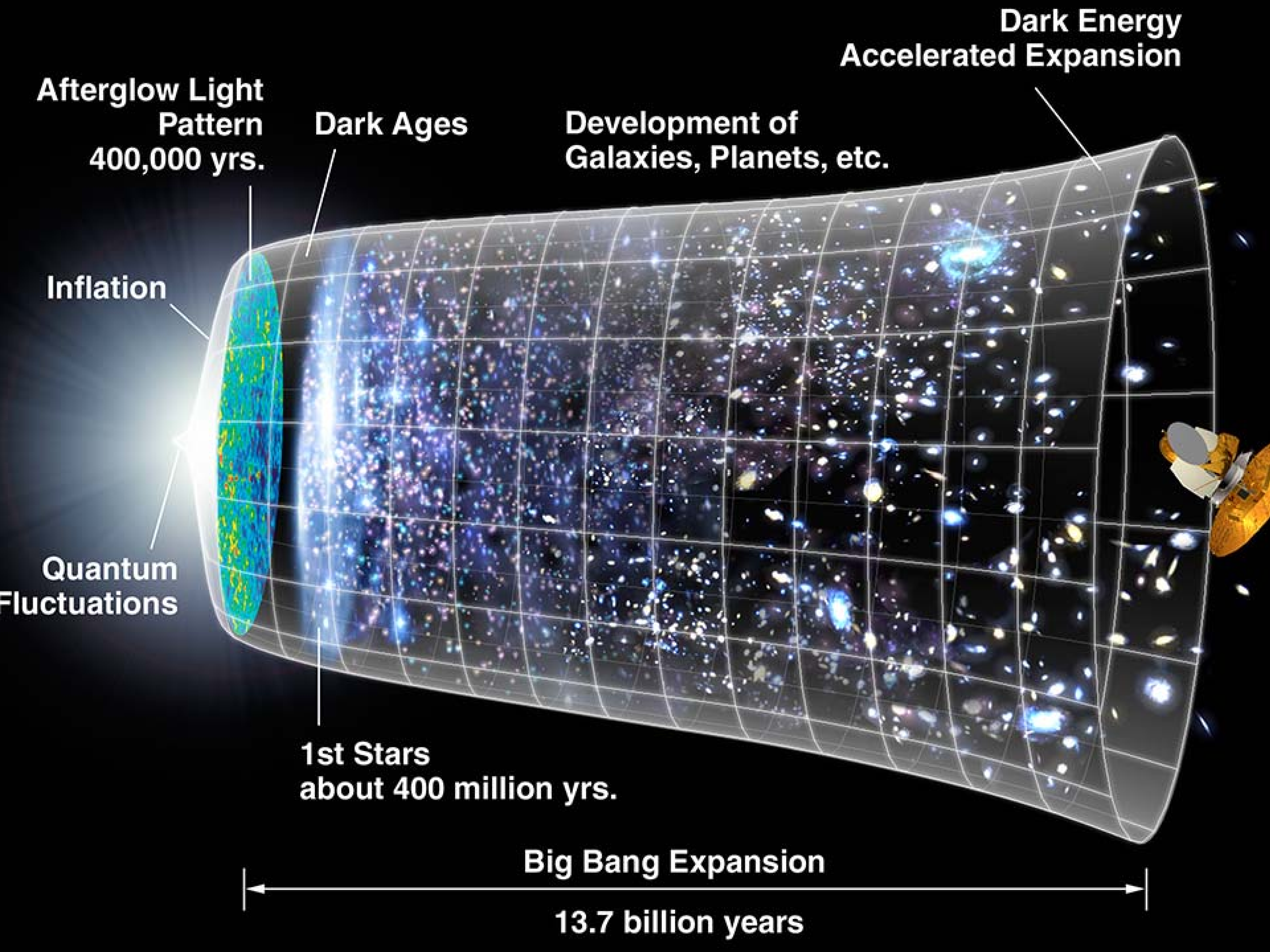

Dark Energy
Accelerated Expansion
Afterglow Light
Pattern
400,000 yrs.
Dark Ages
Development of
Galaxies, Planets, etc.
Inflation
Quantum
Fluctuations
1st Stars
about 400 million yrs.
Big Bang Expansion
13.7 billion years

**THE ENERGY SCALE OF INFLATION IS THE**

**THE SCALE OF GRAVITY IN ITS SEMICLASSICAL REGIME**

**(OR THE SEMICLASSICAL GRAVITY TEMPERATURE )**

**(EQUIVALENT TO THE HAWKING TEMPERATURE)**

**The CMB allows to observe it**
**(while is not possible to observe for Black Holes)**

# CMB Missions Revolutionise Our Understanding of the Universe

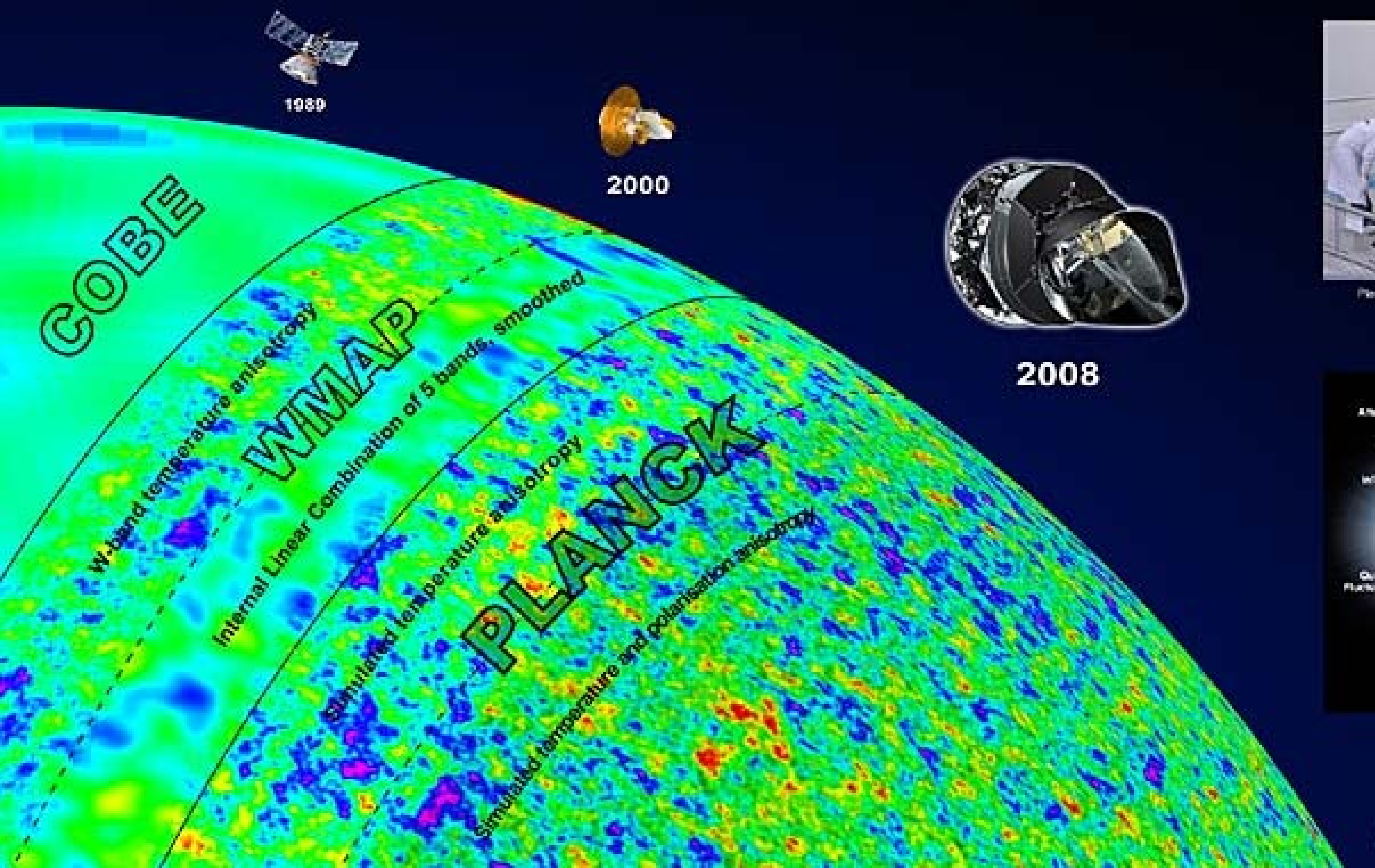

# From WMAP9 to Planck

## Understanding the direction in which data are pointing:

- **PREDICTIONS for Planck**

- **Standard Model of the Universe**
- **Standard Single field Inflation**
- **NO RUNNING of the Primordial Spectral Index**
- **NO Primordial NON GAUSSIANITY**
- **$N_{eff}$ neutrinos : --> Besides meV active neutrinos:**
- **1 or 2 eV sterile neutrinos**
- **Would opens the sterile neutrino Family:**
- **keV sterile neutrino –WDM-**

# Sterile Neutrinos $\nu$

Rhenium and Tritium beta decay (MARE, KATRIN).
Theoretical analysis: H J de V, O. Moreno, E. Moya de Guerra, M. Ramón Medrano, N. Sánchez,
Nucl. Phys. B866, 177 (2013).

[Other possibility to detect a sterile $\nu_s$: a precise measure of nucleus recoil in tritium beta decay.]

Conclusion: the empty slot of right-handed neutrinos in the Standard Model of particle physics can be filled by keV-scale sterile neutrinos describing the DM.

An appealing mass neutrino hierarchy appears:

- Active neutrino: $\sim$ mili eV
- Light sterile neutrino: $\sim$ eV
- Dark Matter: $\sim$ keV
- Unstable sterile neutrino: $\sim$ MeV....

# Sterile neutrinos and CMB fluctuations

CMB data give the effective number of neutrinos, $N_{\rm eff}$.
$N_{\rm eff}$ is related in a subtle way to the number of active neutrinos (3) plus the number of sterile neutrinos.
Planck result: $N_{\rm eff} = 3.5 \pm 0.5$ (95%;P+WP+highL+$H_0$+BAO)

Entropy conservation determines the contributions to $N_{\rm eff}$.
WDM sterile neutrino contribution at recombination

$\Delta N^{WDM} = \left(\frac{T_d}{T_{rc}}\right)^4 = \left[\frac{g_{rc}}{g(T_d)}\right]^{4/3}$. At recombination $g_{rc} = 29/4$.

WDM decouples early at $T_d$ beyond the Fermi scale
The number of UR degrees of freedom at decoupling $g(T_d)$ includes all SM particles and probably beyond.

$g_{SM} = 427/4 \quad , \quad g_{MSSM} = 915/4,$

$\Delta N^{WDM}_{SM} = 0.02771\ldots \quad , \quad \Delta N^{WDM}_{MSSM} = 0.01003\ldots$

Too small to be measurable at present !
Conclusion: Planck results say nothing about WDM.
Besides, Planck results are **compatible** with one or two eV sterile neutrinos (see e. g. G. Steigman, 1303.0049).

# From WMAP9 to Planck

## Understanding the direction in which data are pointing:

- **PREDICTIONS for Planck**

- **Standard Model of the Universe**
- **Standard Single field Inflation**
- **NO RUNNING of the Primordial Spectral Index**
- **NO Primordial NON GAUSSIANITY**
- **$N_{eff}$ neutrinos : --> Besides meV active neutrinos:**
- **1 or 2 eV sterile neutrinos**
- **Would opens the sterile neutrino Family:**
- **keV sterile neutrino –WDM-**

# Effective Theory of Inflation: Ginsburg-Landau Approach

Universal form of the slow-roll inflaton potential:

$V(\phi) = N\, M^4\, w\left(\frac{\phi}{\sqrt{N}\, M_{Pl}}\right)$ , $N \sim 60$ , $\phi =$ inflaton field.

$n_s - 1,\ r =$ order $\frac{1}{N}$ . Running $\frac{dn_s}{d\ln k} \sim \frac{1}{N^2}$.

Primordial Non-Gaussianity $f_{NL} \sim \frac{1}{N}$.

Predictions combining with WMAP+LSS data:

$M = 0.70 \times 10^{16}$ GeV, = energy scale of inflation.

MCMC analysis calls for $w''(\chi) < 0$ at horizon exit

$\Longrightarrow$ double well potential favoured.

$$w(\chi) = \frac{y}{32}\left(\chi^2 - \frac{8}{y}\right)^2$$

Bounds : $r > 0.023\ (95\%\ \mathrm{CL})$ , $r > 0.046\ (68\%\ \mathrm{CL})$

Most probable values: $r \simeq 0.051 \Leftarrow$ measurable by Planck?

quartic coupling $y \simeq 1.26\ldots$ (moderate nonlinearity).

## spectral index $n_s$, the ratio $r$ and the running of $n_s$

$r \equiv$ ratio of tensor to scalar fluctuations.
tensor fluctuations = primordial gravitons.

$$n_s - 1 = -\frac{3}{N} \left[\frac{w'(\chi)}{w(\chi)}\right]^2 + \frac{2}{N} \frac{w''(\chi)}{w(\chi)} \quad , \quad r = \frac{8}{N} \left[\frac{w'(\chi)}{w(\chi)}\right]^2$$

$$\frac{dn_s}{d\ln k} = -\frac{2}{N^2} \frac{w'(\chi)\, w'''(\chi)}{w^2(\chi)} - \frac{6}{N^2} \frac{[w'(\chi)]^4}{w^4(\chi)} + \frac{8}{N^2} \frac{[w'(\chi)]^2\, w''(\chi)}{w^3(\chi)} \, ,$$

$\chi$ is the inflaton field at horizon exit.

$n_s - 1$ and $r$ are always of order $1/N \sim 0.02$ (model indep.)

Running of $n_s$ of order $1/N^2 \sim 0.0003$ (model independent).

Primordial Non-gaussianity $f_{NL} =$ order $1/N$

D. Boyanovsky, H. J. de Vega, N. G. Sanchez,
Phys. Rev. D 73, 023008 (2006), astro-ph/0507595.

# Effective Theory of Inflation (ETI) confirmed by Planck

| Quantity | ETI Prediction | Planck 2013 |
|---|---|---|
| Spectral index $1 - n_s$ | order $1/N = 0.02$ | 0.04 |
| Running $dn_s/dlnk$ | order $1/N^2 = 0.0004$ | $< 0.01$ |
| Non-Gaussianity $f_{NL}$ | order $1/N = 0.02$ | $< 6$ |
| | ETI + WMAP+LSS | |
| tensor/scalar ratio $r$ | r = 0.04-0.05 | $< 0.11$ |
| inflaton potential curvature $V''(0)$ | $V''(0) < 0$ | $V''(0) < 0$ |

ETI + WMAP+LSS means the MCMC analysis combining the ETI with WMAP and LSS data. Such analysis calls for an inflaton potential with negative curvature at horizon exit. The double well potential is favoured (new inflation).
D. Boyanovsky, C. Destri, H. J. de Vega, N. G. Sanchez, arXiv:0901.0549, IJMPA 24, 3669-3864 (2009).

# The Energy Scale of Inflation

Grand Unification Idea (GUT)

- Renormalization group running of electromagnetic, weak and strong couplings shows that they all meet at $E_{GUT} \simeq 2 \times 10^{16}$ GeV
- Neutrino masses are explained by the see-saw mechanism: $m_\nu \sim \frac{M^2_{\rm Fermi}}{M_R}$ with $M_R \sim 10^{16}$ GeV.
- Inflation energy scale: $M \simeq 10^{16}$ GeV.

Conclusion: the GUT energy scale appears in at least three independent ways.

Moreover, moduli potentials: $V_{moduli} = M^4_{\rm SUSY} \; v\left(\frac{\phi}{M_{Pl}}\right)$

ressemble inflation potentials provided $M_{\rm SUSY} \sim 10^{16}$ GeV.
First observation of SUSY in nature??

# MCMC Results for Trinomial New Inflation.

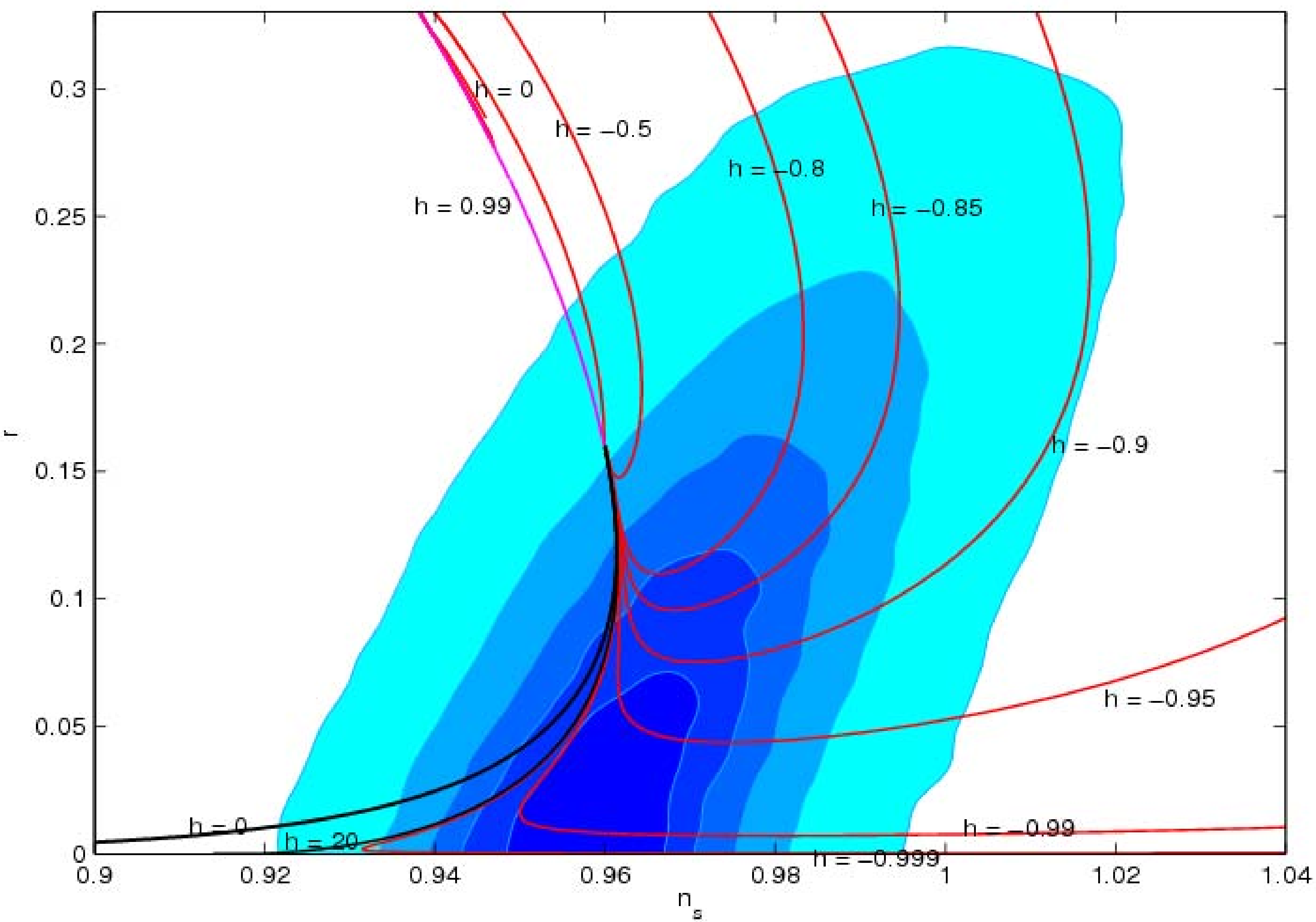

# LOWER BOUND on r

# THE PRIMORDIAL GRAVITONS

Our theory input (Effective Theory Inflation) in the MCMC data analysis of WMAP5+LSS+SN data).

C. Destri, H J de Vega, N G Sanchez, Phys Rev D77, 043509 (2008) shows:

Besides the upper bound for r (tensor to scalar ratio) $r < 0.22$, we find a clear peak in the r distribution and we obtain a lower bound

$$r > 0.023 \text{ at } 95\% \text{ CL and}$$

$$r > 0.046 \text{ at } 68\% \text{ CL.}$$

Moreover,we find $r = 0.051$ the most probable value

For the other cosmological parameters, both analysis agree.

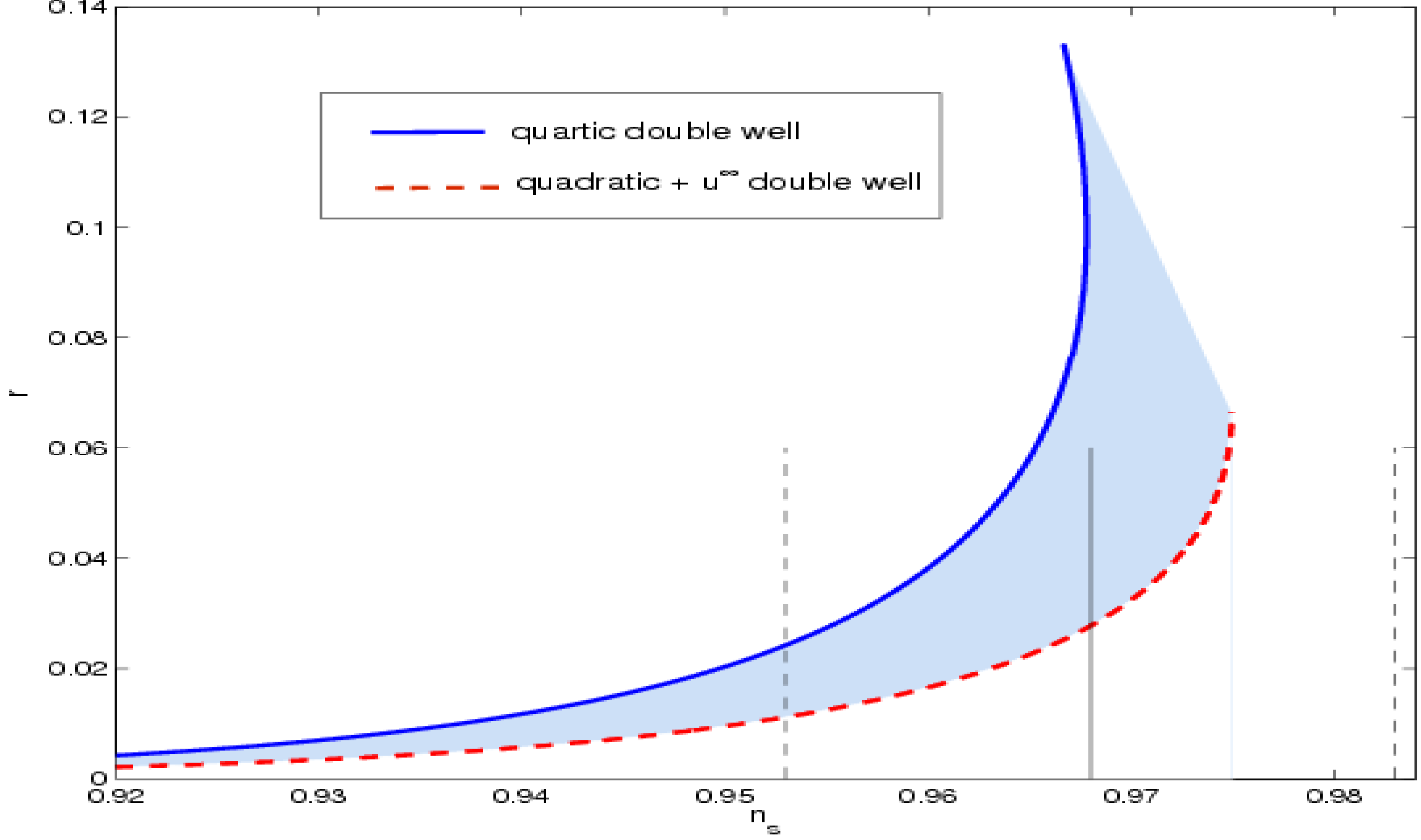


# THE PRIMORDIAL COSMIC BANANA

**The tensor to scalar ratio r (primordial gravitons) versus the scalar spectral index n_s. The amount of r is always non zero**
**H.J. de Vega, C. Destri, N.G. Sanchez, Annals Phys 326, 578(2011)**

# WMAP 5 years data set plus other CMB data

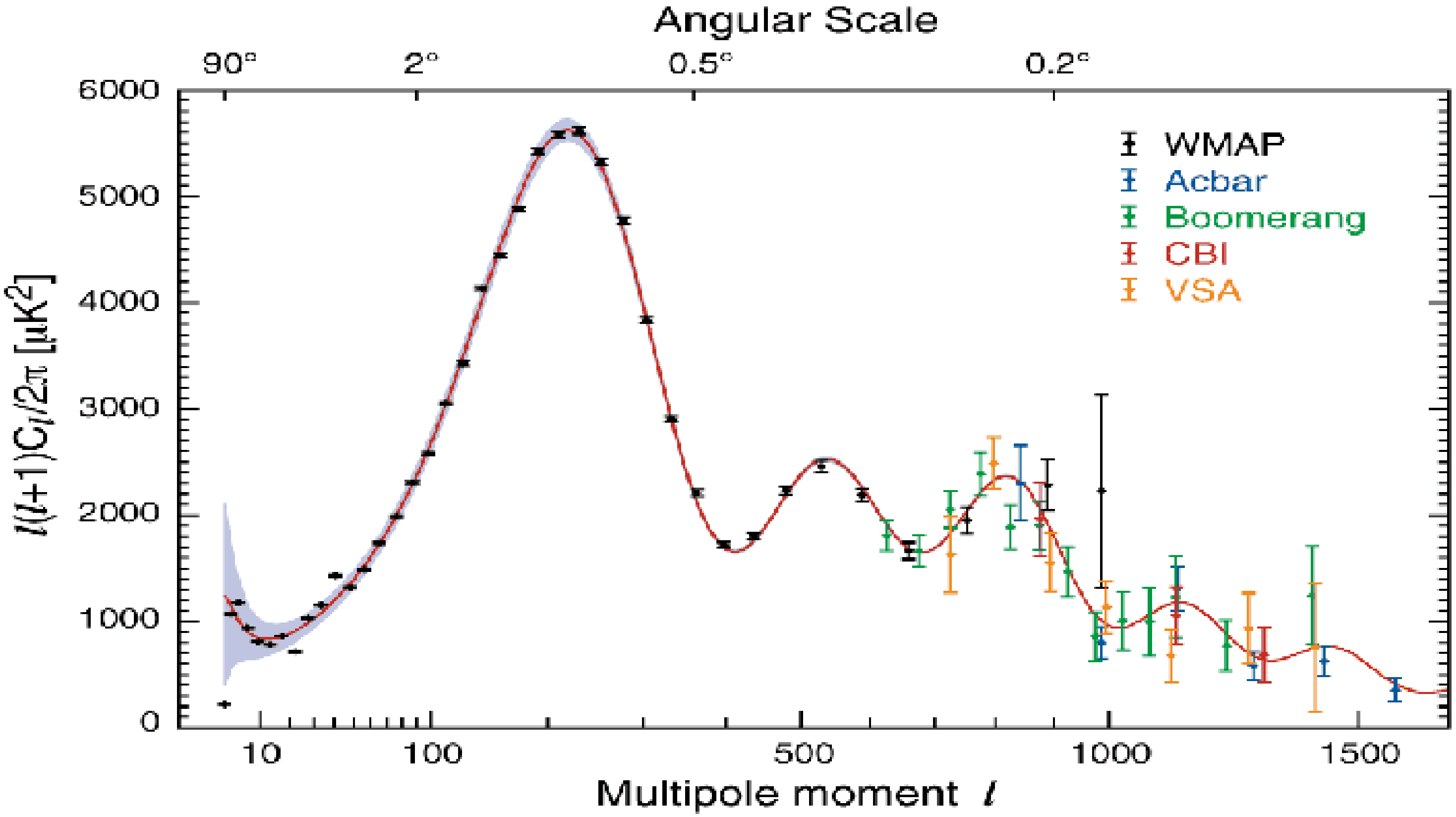


These Acoustic Oscillations are excited by the primordial inflationary power: $P(k) = \Delta\, k^{n_s - 1}, \; n_s =$ spectral index. An explanation for the the quadrupole suppression: the fast-roll stage of inflation. DB, HJdV, NGS, PRD74, 123006 and 123007 (2006).

# Fast roll Inflation produces the Observed Quadrupole CMB Suppression

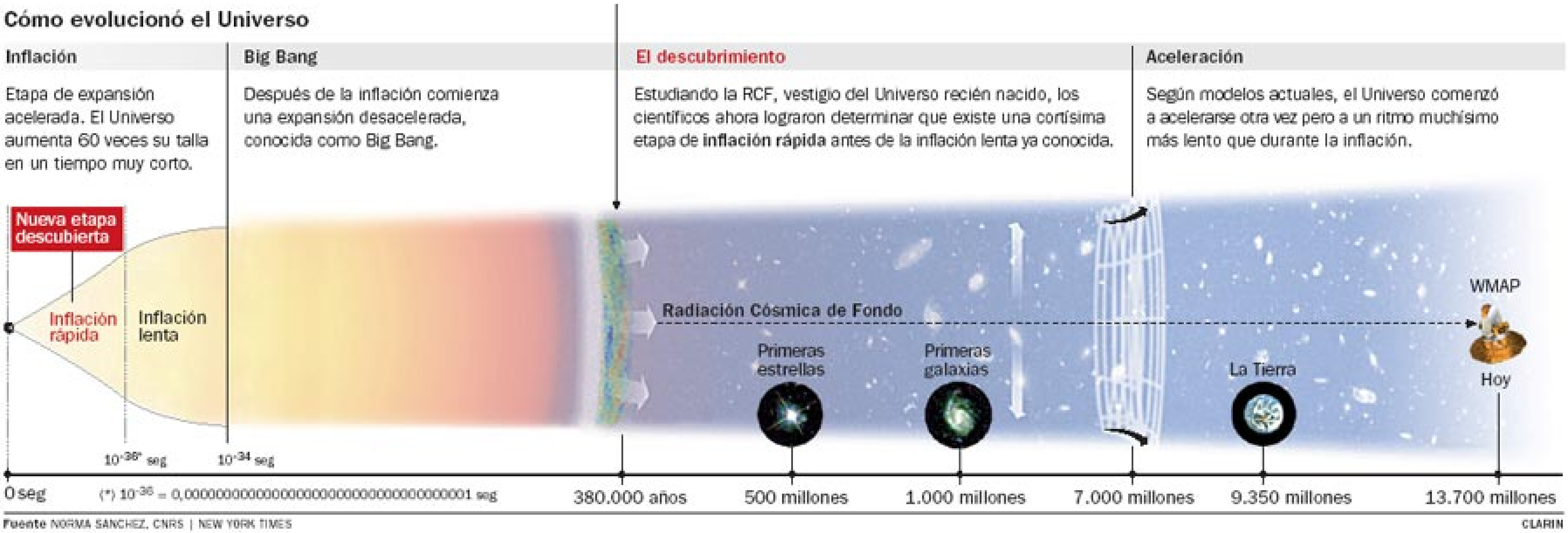


**D. Boyanovsky, H. J de Vega and N. G. Sanchez,**

**” CMB quadrupole suppression II : The early fast roll stage ”**

**Phys. Rev. D74 , 123006 (2006)**

## Comparison, with the experimental WMAP5 data

of the theoretical $C_\ell^{TT}$ multipoles

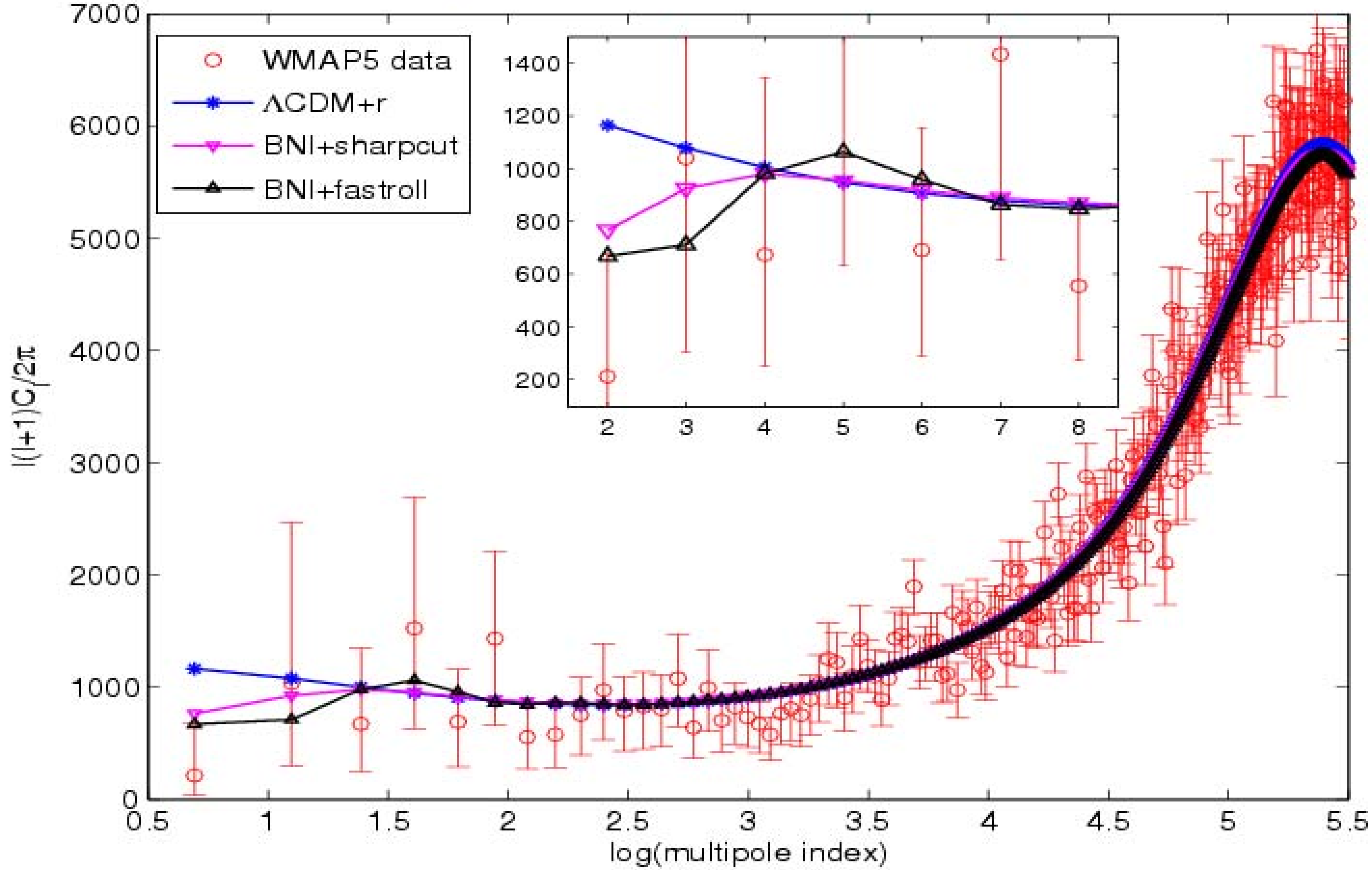

# • Large Hadron Collider

- The first LHC results at 7-8 TeV, with the discovery of a candidate Higgs boson and the non observation of new particles or exotic phenomena, have made a big step towards completing the experimental confirmation of the Standard Model of particle physics.

- It is thus a good moment to recall our scientific predictions made several years ago on this matter because they are of full actuality.

# Large Hadron Collider - LHC-

**The results are completely in line with the Standard Model.**

**No evidence of SUSY at LHC**

**"*Supersymmetry may not be dead but these latest results have certainly put it into hospital.*"**

**(Prof Chris Parkes, spokesperson for the UK Participation in the LHCb experiment)**

**→Does Not support wimps -CDM-**

***(In agreement with all dedicated wimp experiments at work from more than 20 years which have not found any wimp's signal )*** **"So far researchers who are racing to find evidence of so called "new physics", ie non-standard models, have run into a series of dead ends".**

# ANTIMATTER IN SPACE - AMS on board ISS Alpha Magnet Spectrometer


NASA

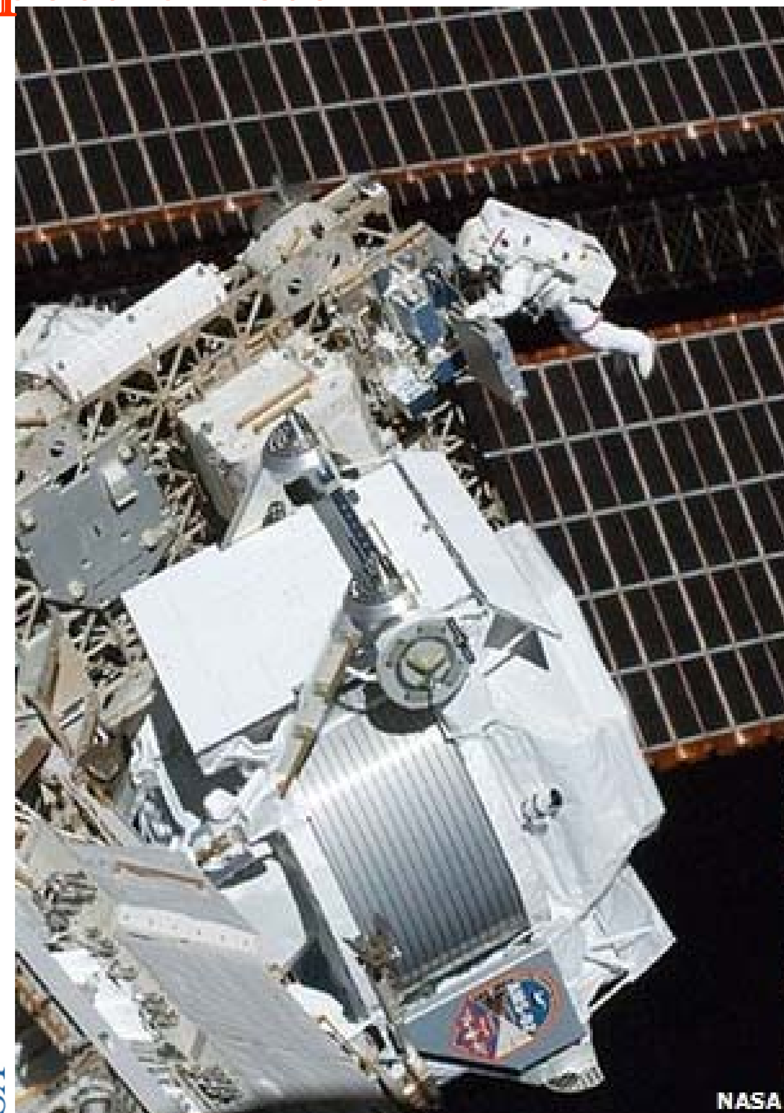

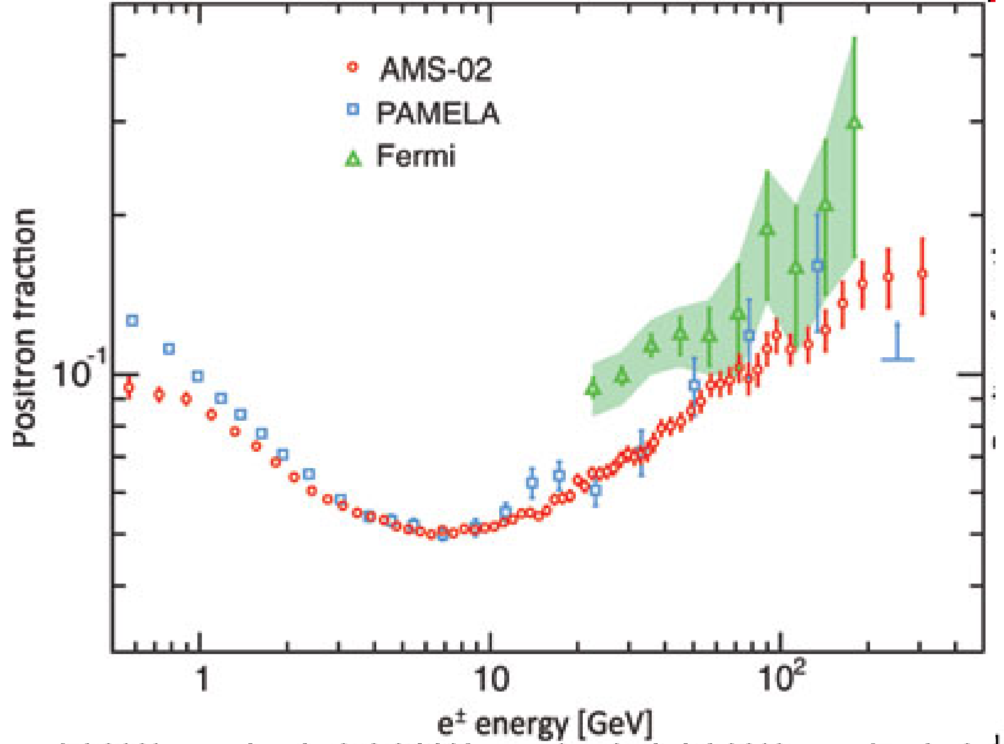


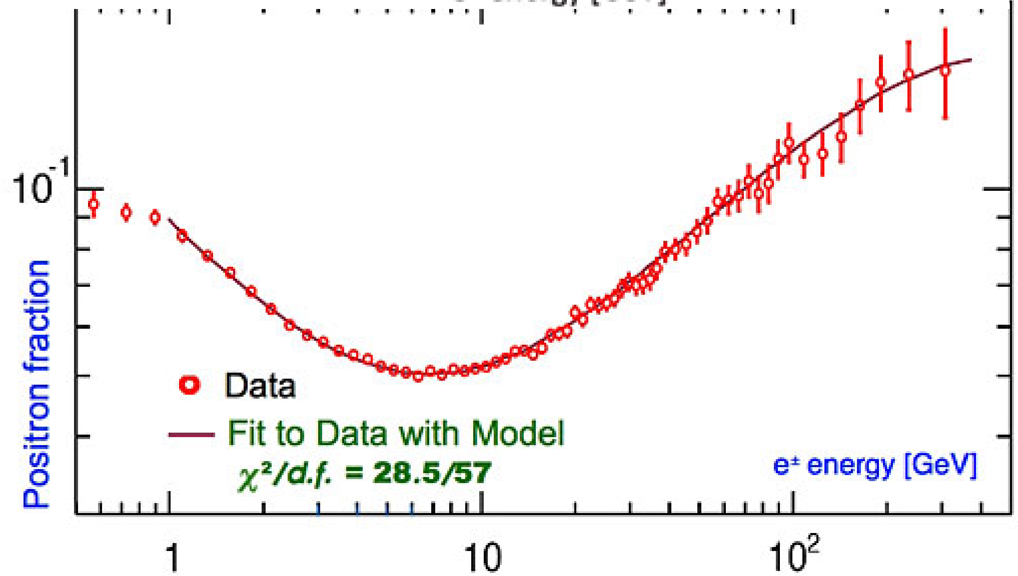


**Positron excess in cosmic rays are not related to DM physics but to astrophysical sources and astrophysical mechanisms and can be explained by them**

**LHC**

**AMS**

**PLANCK**

Three beautiful and big experiments of performant instruments, technology, industry, achievements and successful operation which do not find the main scientific objective emphasized by them (for which they were designed)

- **Why No Experimental Detection of the DM particle has been reached so far ?**
- **Because:**
- All experimental searches for DM particles are dedicated to CDM: wimps of m > 1 GeV,
- While the DM particle mass is in the keV scale .
- Moreover, past, present and future reports of signals of such CDM experiments **cannot be due to DM** because of the same reason.
- **The inconclusive signals in such experiments should be originated by phenomena of other kinds.**
- In addition, such signals contradict each other supporting the idea that they are **unrelated to any DM detection.**

# Direct searches of CDM particles

All direct searches of wimps look for $m \gtrsim 1$ GeV.

Past, present and future reports of signals in such wimp experiments cannot be due to DM detection because the DM particle mass is in the keV scale.

The inconclusive signals in such experiments should be originated by other kinds of phenomena.

Contradictions between supposed detection signals in DAMA, CDMS-II, CoGeNT, CRESST, XENON100.

CONCLUSION: These signals are unrelated to DM.

$e^+$ and $\bar{p}$ excess in cosmic rays reported by Pamela and Fermi may be explained by astrophysics: P. L. Biermann et al. PRL (2009), P. Blasi, P. D. Serpico PRL (2009).

AMS02: precise measure of the positron fraction in Galactic cosmic rays (CR) (PRL 2013) that increases with energy.

Blum, Katz & Waxman (arXiv:1305.1324) show that this is consistent with positron production by the collision of high energy primary CR with the interstellar medium.

# Dark Matter Particles

DM particles decouple due to the universe expansion, their distribution function freezes out at decoupling.

The characteristic length scale is the free streaming scale (or Jeans' scale). For DM particles decoupling UR:

$r_{Jeans} = 57.2 \, \mathrm{kpc} \, \frac{\mathrm{keV}}{m} \left(\frac{100}{g_d}\right)^{\frac{1}{3}}$, solving the linear Boltz-V eqs.

$g_d =$ number of UR degrees of freedom at decoupling.

DM particles can freely propagate over distances of the order of the free streaming scale.

Therefore, structures at scales smaller or of the order of $r_{Jeans}$ are erased.

The size of the DM galaxy cores is in the $\sim 50$ kpc scale $\Rightarrow \; m$ should be in the keV scale (WDM particles).

For neutrinos $m \sim$ eV HDM particles
$r_{Jeans} \sim 60$ Mpc $\Rightarrow$ NO GALAXIES FORMED.

# The Free Streaming Scale

The characteristic length scale is the free streaming scale (or Jeans' scale)

$$r_{lin} = 2\sqrt{1+z_{eq}} \left( \frac{3\, M_{Pl}^2}{H_0 \sqrt{\Omega_{DM}}\, Q_{prim}} \right)^{\frac{1}{3}} = 21.1\, q_p^{-\frac{1}{3}} \text{ kpc}$$

$q_p \equiv Q_{prim}/(\mathrm{keV})^4$. DM particles can freely propagate over distances of the order of the free streaming scale.

$$r_{lin} = 57.2\, \mathrm{kpc}\, \frac{\mathrm{keV}}{m} \left( \frac{100}{g_d} \right)^{\frac{1}{3}}$$

Therefore, structures at scales smaller or of the order $r_{lin}$ are erased.

It is useful to introduce the dimensionless wavenumbers:

$$\gamma \equiv k\, r_{lin}/\sqrt{3} \quad \text{and} \quad \alpha \equiv \sqrt{3}\,\gamma/\sqrt{I_4}$$

where $I_4$ is the second momentum of the DM zeroth order distribution.

# Mass Estimates for DM particles

Combining the previous expressions lead to general formulas for $m$ and $g_d$:

$$m = 0.2504\,\mathrm{keV}\ \left(\frac{Z}{g}\right)^{\frac{1}{4}} \frac{\left[\int_0^\infty y^4\ F_d(y)\ dy\right]^{\frac{3}{8}}}{\left[\int_0^\infty y^2\ F_d(y)\ dy\right]^{\frac{5}{8}}}$$

$$g_d = 35.96\, Z^{\frac{1}{4}}\ g^{\frac{3}{4}}\ \left[\int_0^\infty y^4\ F_d(y)\ dy\ \int_0^\infty y^2\ F_d(y)\ dy\right]^{\frac{3}{8}}$$

These formulas yield for relics decoupling UR at LTE:

$$m = \left(\frac{Z}{g}\right)^{\frac{1}{4}}\ \mathrm{keV} \left\{ \begin{array}{l} 0.568 \\ 0.484 \end{array} \right. ,\ g_d = g^{\frac{3}{4}}\ Z^{\frac{1}{4}} \left\{ \begin{array}{ll} 155 & \mathrm{Fermions} \\ 180 & \mathrm{Bosons} \end{array} \right. .$$

Since $g = 1 - 4$, we see that $g_d > 100 \Rightarrow T_d > 100$ GeV.

$1 < Z^{\frac{1}{4}} < 5.6$ for $1 < Z < 1000$. Example: for DM Majorana fermions $(g = 2)$ $m \simeq 0.85$ keV.

## he Phase-space density $Q = \rho/\sigma^3$ and its decrease factor

The phase-space density today $Q_{today}$ follows observing dwarf spheroidal satellite galaxies of the Milky Way (dSphs) as well as spiral galaxies. Its value is galaxy dependent.

For dSphs $Q_{today} \sim 5000 \, (0.18 \text{ keV})^4$ Gilmore et al. 07/08.

During structure formation $Q$ decreases by a factor that we call $Z$, $(Z > 1)$ : $\quad Q_{today} = \frac{1}{Z} \, Q_{prim}$

The spherical model gives $Z \simeq 41000$ and $N$-body simulations indicate: $10000 > Z > 1$. $Z$ is galaxy dependent.

As a consequence $m$ is in the keV scale:
1 keV $\lesssim m \lesssim 10$ keV.

This is true both for DM decoupling in or out of equilibrium, bosons or fermions.
It is independent of the particle physics model.

# CDM free streaming scale

For CDM particles with $m \sim 100$ GeV: $r_{lin} \sim 0.1$ pc

Hence CDM structures keep forming till scales as small as the solar system.

This has been explicitly verified by all CDM simulations but never observed in the sky.

There is over abundance of small structures in CDM (also called the satellite problem).

# CDM free streaming scale

For CDM particles with $m \sim 100$ GeV $\Rightarrow$ $r_{Jeans} \sim 0.1$ pc.

Hence CDM structures keep forming till scales as small as the solar system.

This is a robust result of $N$-body CDM simulations but never observed in the sky.

There is over abundance of small structures in CDM (also called the satellite problem).

CDM has many serious conflicts with observations:

Galaxies naturally grow through merging in CDM models.

Observations show that galaxy mergers are rare ($< 10\%$).

Pure-disk galaxies (bulgeless) are observed whose formation through CDM is unexplained.

CDM predicts cusped density profiles: $\rho(r) \sim 1/r$ for small $r$.

Observations show cored profiles: $\rho(r)$ bounded for small $r$.

# Dark Matter: from primordial fluctuations to Galaxies

❖ **Cold** **(CDM): small velocity dispersion:** **small structures form first, bottom-up hierarchical growth formation,** ***too heavy (GeV)***

❖**Hot** **(HDM) : large velocity dispersion:** **big structures form first, top-down, fragmentation, ruled out,** ***too light*** **(eV)**

**Warm** **(WDM): ``in between", *right mass scale,* (keV)**

## *ΛWDM* Concordance Model:

***CMB + LSS + SSS Observations***

***DM is WARM and COLLISIONLESS***

***CDM Problems*:**

- "clumpy halo problem", large number of satellite galaxies
  "satellite problem", overabundance of small structures
- $\rho$ (r) ~ 1 / r (cusp)
- And other problems…..

# WDM properties

WDM is characterized by

- its initial power spectrum cutted off for scales below $\sim 50$ kpc. Thus, structures are not formed in WDM for scales below $\sim 50$ kpc.
- its initial velocity dispersion. However, this is negligible for $z < 20$ where the non-linear regime starts.
- Classical $N$-body simulations break down at small distances ( $\sim$ pc). Need of quantum calculations to find WDM cores.

Structure formation is hierarchical in CDM.

WDM simulations show in addition top-hat structure formation at large scales and low densities but hierarchical structure formation remains dominant.

# Structure Formation in the Universe

Structures in the Universe as galaxies and cluster of galaxies form out of the small primordial quantum fluctuations originated by inflation just after the big-bang.

These linear small primordial fluctuations grow due to gravitational unstabilities (Jeans) and then classicalize.

Structures form through non-linear gravitational evolution.

Hierarchical formation starts from small scales first.

$N$-body CDM simulations fail to produce the observed structures for small scales less than some kpc.

Both $N$-body WDM and CDM simulations yield identical and correct structures for scales larger than some kpc.

WDM predicts correct structures for small scales (below kpc) when its quantum nature is taken into account.

Primordial power $P(k)$: first ingredient in galaxy formation.

# Linear primordial power today $P(k)$ vs. $k$ Mpc $h$

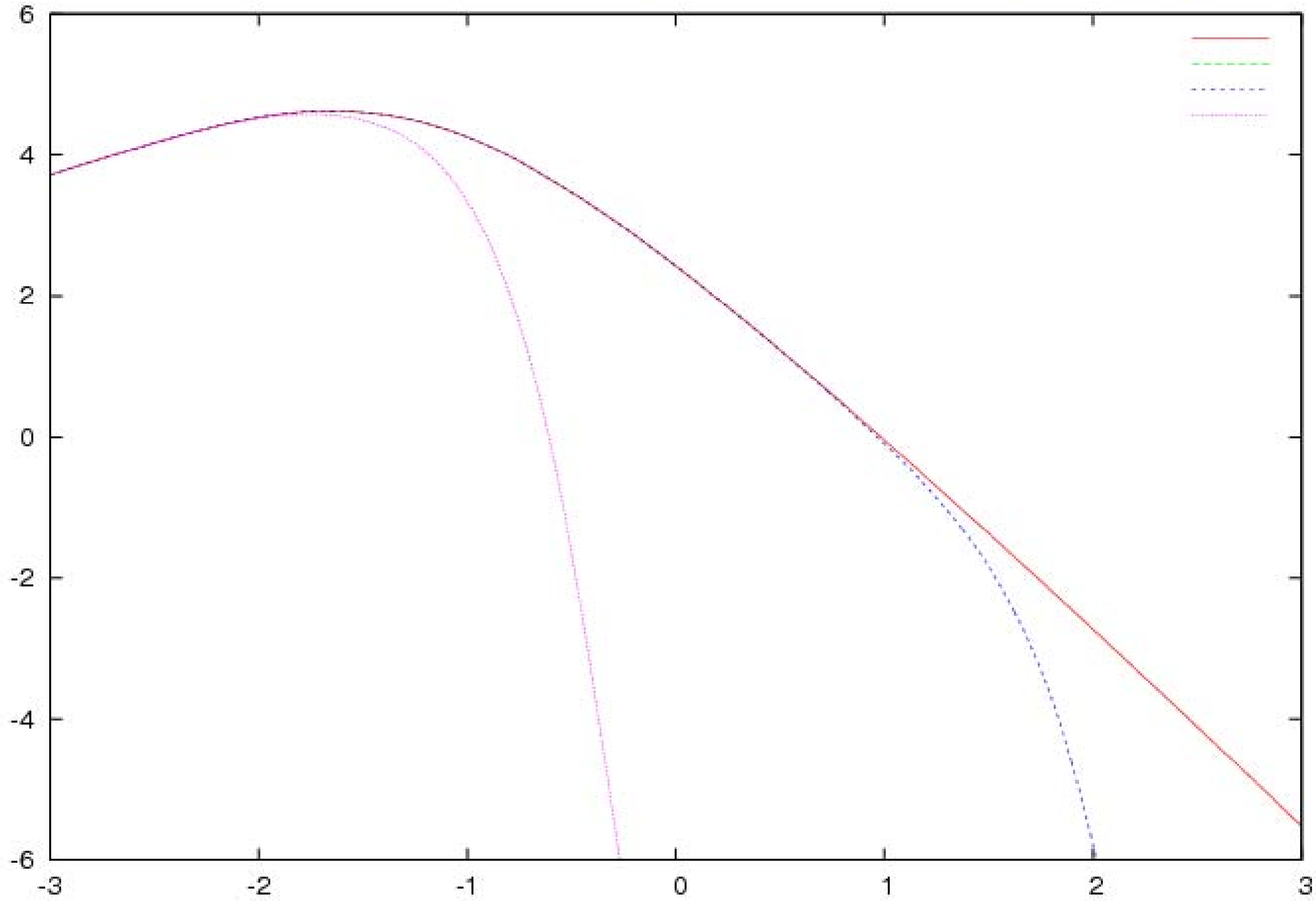


$\log_{10} P(k)$ vs. $\log_{10}[k \text{ Mpc } h]$ for WIMPS, 1 keV DM particles and 10 eV DM particles. $P(k) = P_0 \, k^{n_s} \, T^2(k)$.

$P(k)$ cutted for 1 keV DM particles on scales $\lesssim 100$ kpc.

Transfer function in the MD era from Gilbert integral eq.

# Linear primordial power today $P(k)$ vs. $k$ Mpc $h$

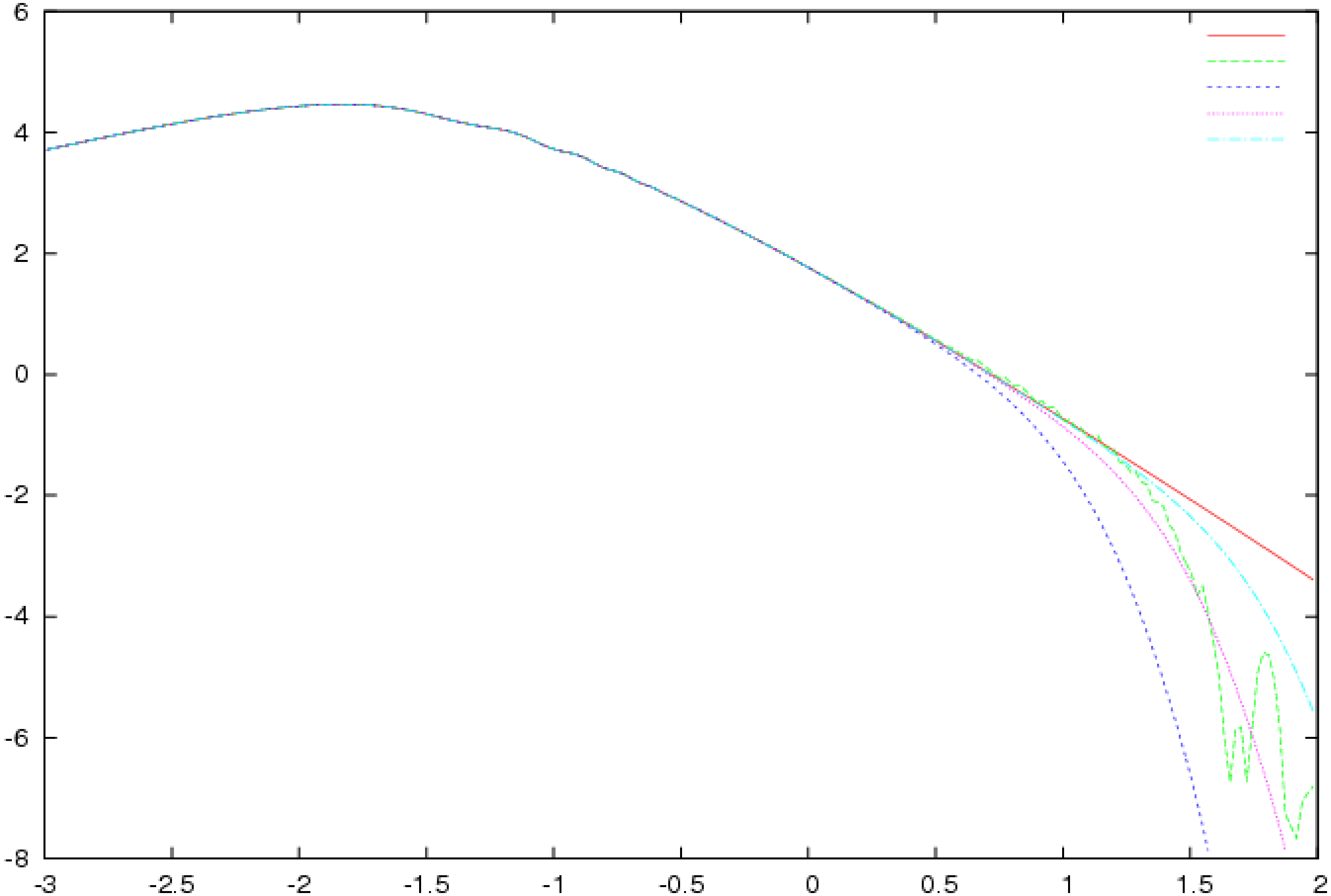


$\log_{10} P(k)$ vs. $\log_{10}[k \text{ Mpc } h]$ for CDM, 1 keV, 2 keV, light-blue 4 keV DM particles decoupling in equil, and 1 keV sterile neutrinos. WDM cuts $P(k)$ on small scales $r \lesssim 100 \, (\text{keV}/m)^{4/3}$ kpc. CDM and WDM identical for CMB.

# Sterile neutrino models

- DW: Dodelson-Widrow model (1994) sterile neutrinos produced by non-resonant mixing from active neutrinos.
- Shi-Fuller model (1998) sterile neutrinos produced by resonant mixing from active neutrinos.
- $\nu$-MSM model (1981)-(2006) sterile neutrinos produced by a Yukawa coupling from a real scalar $\chi$.
- DM models must reproduce $\bar{\rho}_{DM}$, galaxy and structure formation and be consistent with particle experiments.

WDM particles in different models behave just as if their masses were different (FD = thermal fermions):

$$\frac{m_{DW}}{\mathrm{keV}} \simeq 2.85 \left(\frac{m_{FD}}{\mathrm{keV}}\right)^{\frac{4}{3}}, \; m_{SF} \simeq 2.55 \; m_{FD}, \; m_{\nu\mathrm{MSM}} \simeq 1.9 \; m_{FD}.$$

H J de Vega, N Sanchez,
Phys. Rev. D85, 043516 and 043517 (2012).

# WDM vs. CDM linear fluctuations today

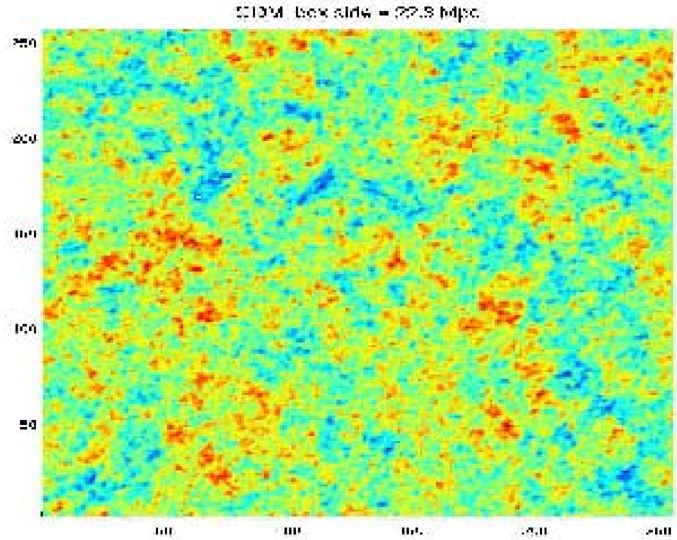

Box side = 22.6 Mpc. [C. Destri, private communication].

WDM:

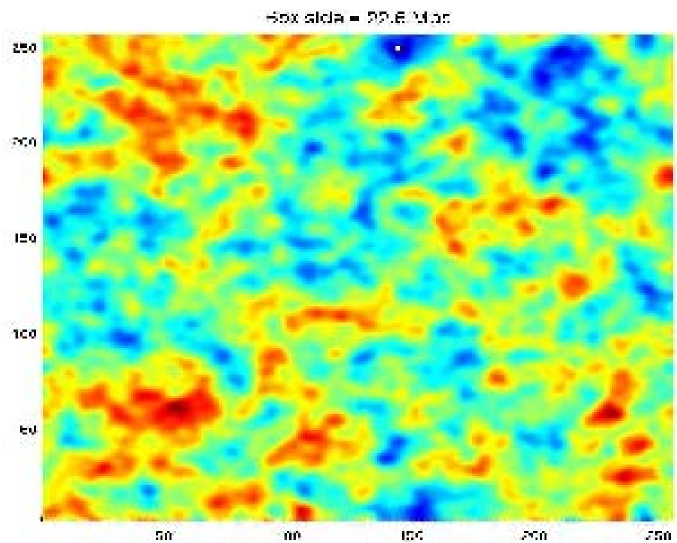

# The expected overdensity

The expected overdensity within a radius $R$ in the linear regime

$\sigma^2(R) = \int_0^\infty \frac{dk}{k}\, \Delta^2(k)\, W^2(kR) \quad , \quad W(kR)$ : window function.

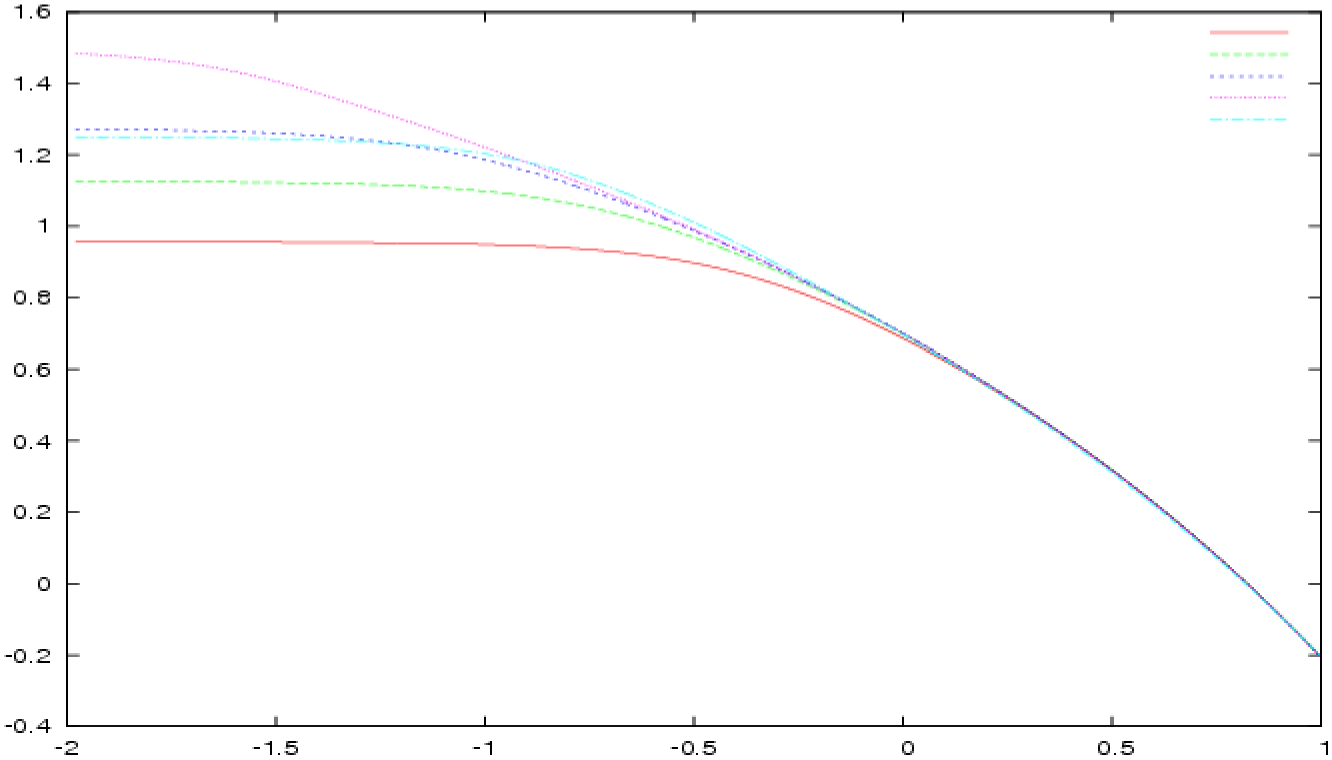


$\log \sigma(R)$ vs. $\log R$ for CDM, 1 keV, 2 keV, 4 keV DM particles decoupling in equil, and 1 keV (light-blue) sterile neutrinos. WDM flattens and reduces $\sigma(R)$ for small scales.

# The Mass function

The differential mass function gives the number of isolated bounded structures with mass between $M$ and $M + dM$: (Press-Schechter)

$$\frac{dN}{dM} = -\frac{2\,\delta_c}{\sqrt{2\,\pi}\;\sigma^2(M,z)}\;\frac{\rho_M(z)}{M^2}\;\frac{d\sigma(M,z)}{d\ln M}\;e^{-\delta_c^2/[2\,\sigma^2(M,z)]},$$

$\delta_c = 1.686\ldots$: linear estimate for collapse from the spherical model.

$\sigma(M, z)$ is constant for WDM for small scales: small objects (galaxies) formation is suppresed in WDM in comparison with CDM.

$$\sigma(M, z) = \frac{g(z)}{z+1}\;\sigma(M, 0)$$

$g(z)$: takes into account the effect of the cosmological constant, $g(0) = 0.76\;,\;\; g(\infty) = 1$

$(M^2/\rho) \log d\sigma(M,z)/d\ln M$ **vs.** $\log_{10} M/M_\odot$

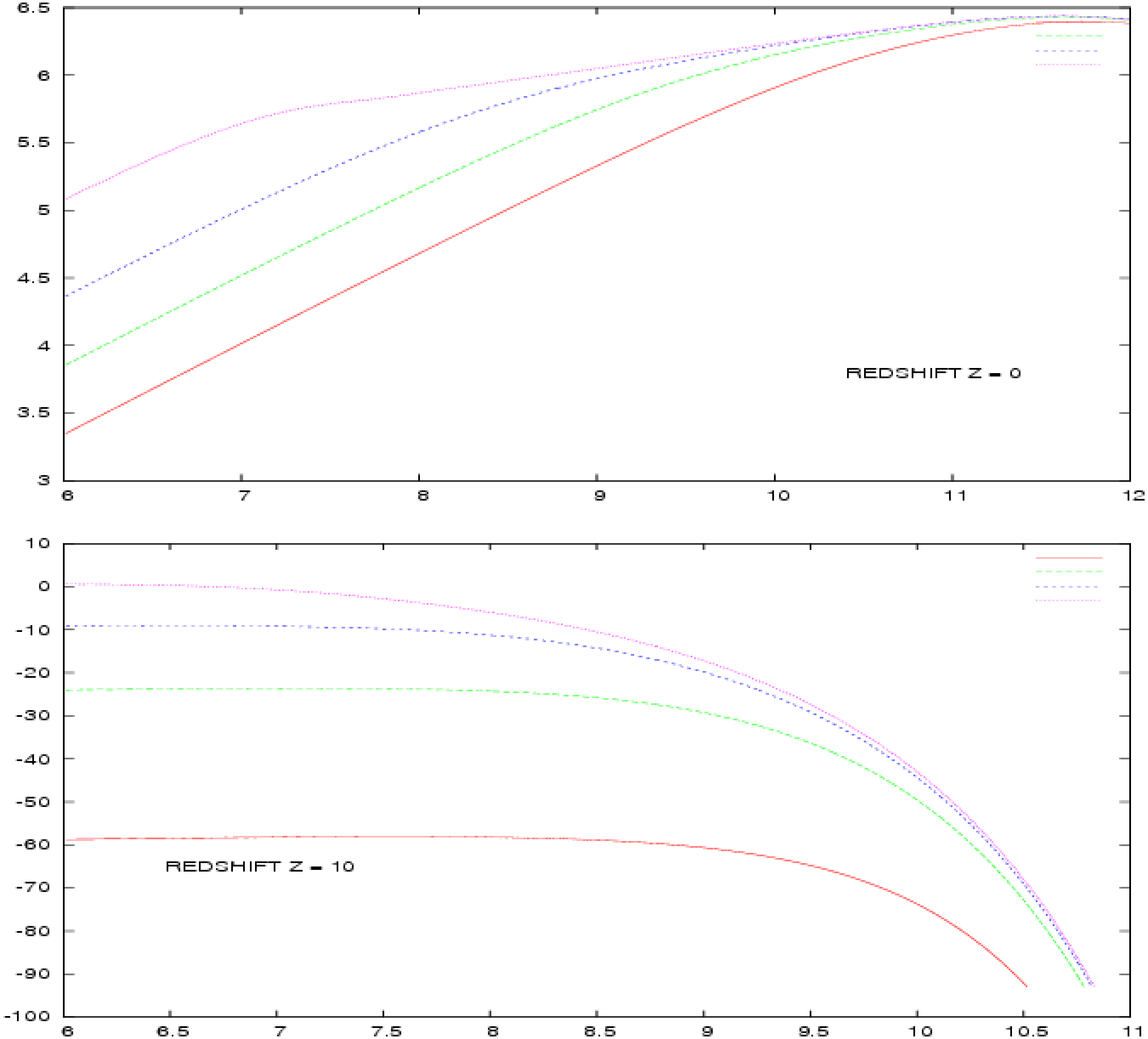


CDM, 1 keV, 2 keV, 4 keV WDM decoupling in equilibrium.

# Linear and non-linear regimes in z and R

$\sigma^2(R, z) \sim 1$: borderline between linear and non-linear regimes. Objects (galaxies) of scale R and mass $\sim R^3$ start to form when this scale becomes non-linear.
Smaller objects form earlier.

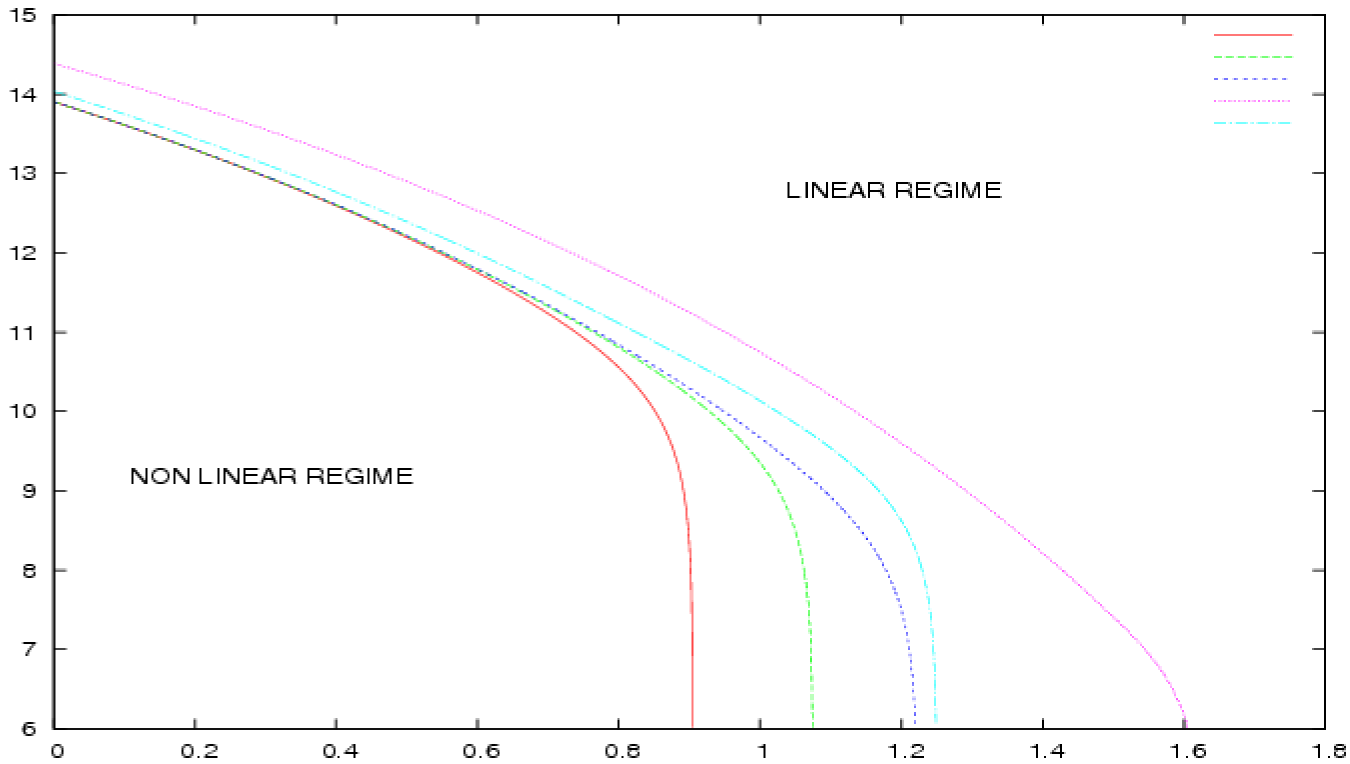


$\log M/M_\odot$ vs. $\log(z+1)$ for CDM, 1 keV, 2 keV, 4 keV DM particles decoupling in equil, and 1 keV (light-blue) sterile $\nu$.

# Velocity widths in galaxies

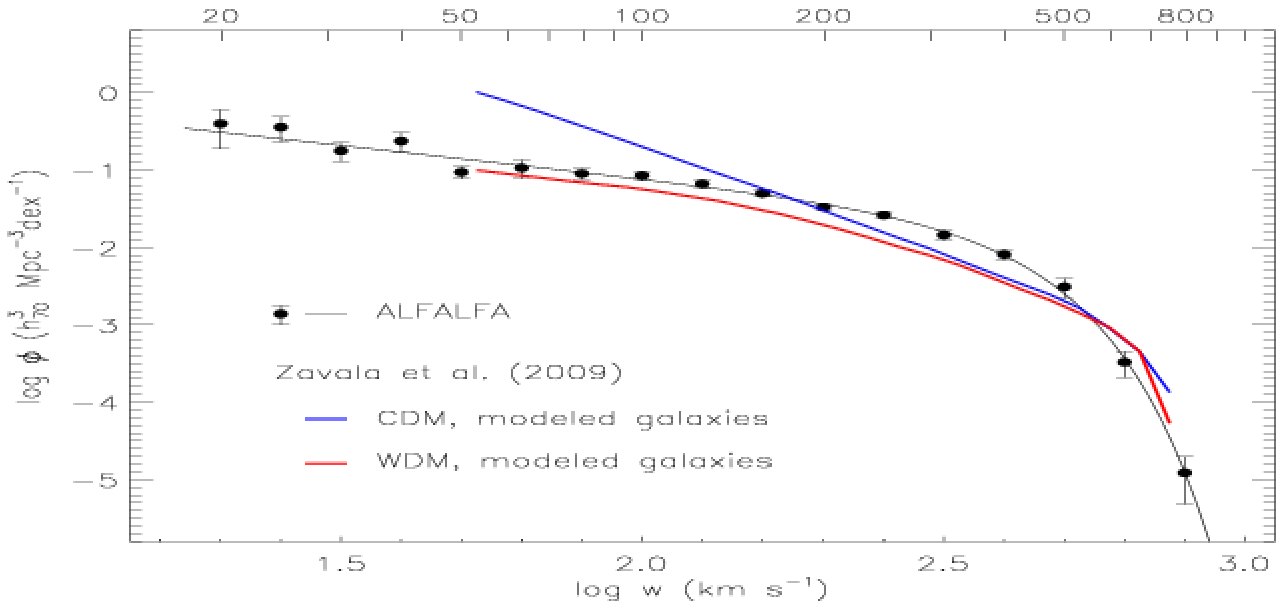


Velocity widths in galaxies from 21cm HI surveys. ALFALFA survey clearly favours WDM over CDM. (Papastergis et al. 2011, Zavala et al. 2009).

Notice that the WDM red curve is for $m = 1$ keV WDM particle decoupling at thermal equilibrium.

The 1 keV WDM curve falls somehow below the data suggesting a slightly larger WDM particle mass.

# The constant surface density in DM and luminous galax

The Surface density for dark matter (DM) halos and for luminous matter galaxies defined as: $\mu_{0D} \equiv r_0 \, \rho_0,$

$r_0 =$ halo core radius, $\rho_0 =$ central density for DM galaxies

$$\mu_{0D} \simeq 120 \, \frac{M_\odot}{\mathrm{pc}^2} = 5500 \, (\mathrm{MeV})^3 = (17.6 \, \mathrm{Mev})^3$$

5 kpc < $r_0$ < 100 kpc. For luminous galaxies $\rho_0 = \rho(r_0)$. Donato et al. 09, Gentile et al. 09.[$\mu_{0D} = g$ in the surface].

Universal value for $\mu_{0D}$: independent of galaxy luminosity for a large number of galactic systems (spirals, dwarf irregular and spheroidals, elliptics) spanning over $14$ magnitudes in luminosity and of different Hubble types.

Similar values $\mu_{0D} \simeq 80 \, \frac{M_\odot}{\mathrm{pc}^2}$ in interstellar molecular clouds of size $r_0$ of different type and composition over scales $0.001 \, \mathrm{pc} < r_0 < 100$ pc (Larson laws, 1981).

# DM surface density from linear Boltzmann-Vlasov eq

The distribution function of the decoupled DM particles:

$f(\vec{x}, \vec{p}; t) = g\ f_0^{DM}(p) + F_1(\vec{x}, \vec{p}; t)$ , $f_0^{DM}(p) =$ zeroth order DM distribution function in or out of thermal equilibrium.

We evolve the distribution function $F_1(\vec{x}, \vec{p}; t)$ according to the linearized Boltzmann-Vlasov equation since the end of inflation. The DM density fluctuations are given by

$$\Delta(t, \vec{k}) \equiv m \int \frac{d^3p}{(2\pi)^3} \int d^3x\, e^{-i\,\vec{x}\cdot\vec{k}}\, F_1(\vec{x}, \vec{p}; t)$$

Today: $\Delta(\mathrm{today}, \vec{k}) = \rho_{DM}\ \bar{\Delta}(z = 0, k)\ \sqrt{V}\ |\phi_k|\ g(\vec{k})$ ,

where $\bar{\Delta}(z, k)$ obeys a Volterra integral equation,

the primordial inflationary fluctuations are:

$|\phi_k| = \sqrt{2}\ \pi\ \frac{|\Delta_0|}{k^{\frac{3}{2}}}\ \left(\frac{k}{k_0}\right)^{\frac{n_s - 1}{2}}$ , $g(\vec{k})$ is a random gaussian field,

$V =$ phase-space volume at horizon re-entering

$|\Delta_0| \simeq 4.94\ 10^{-5},\ n_s \simeq 0.964,\ k_0 = 2\ \mathrm{Gpc}^{-1}$ , WMAP7 .

# Density profiles in the linear approximation

Density profiles turn to be cored at scales $r \ll r_{lin}$.

Intermediate regime $r \gtrsim r_{lin}$:

$$\rho_{lin}(r) \overset{r \gtrsim r_{lin}}{=} c_0 \left(\frac{r_{lin}}{r}\right)^{1+n_s/2} \rho_{lin}(0) \quad , \quad 1 + n_s/2 = 1.482.$$

$\rho_{lin}(r)$ scales with the primordial spectral index $n_s$.

The theoretical linear results agree with the universal empirical behaviour $r^{-1.6 \pm 0.4}$: M. G. Walker et al. (2009) (observations), I. M. Vass et al. (2009) (simulations).

The agreement between the linear theory and the observations is remarkable.

In the asymptotic regime $r \gg r_{lin}$ the small k behaviour of $\Delta(k, t_{\text{today}}) \overset{k \to 0}{=} c_1 \, (k \, r_{lin})^s$ with $s \simeq 0.5$ implies the presence of a tail: $\rho_{lin}(r) \overset{r \gg r_{lin}}{\simeq} c \left(\frac{r_{lin}}{r}\right)^2$.

# Wimps vs. galaxy observations

| | Observed Values | Wimps in linear theory |
|---|---|---|
| $r_0$ | 5 to 52 kpc | $0.045$ pc |
| $\rho_0$ | $1.57$ to $19.3 \times 10^{-25}\ \frac{\mathrm{g}}{\mathrm{cm}^3}$ | $0.73 \times 10^{-14}\ \frac{\mathrm{g}}{\mathrm{cm}^3}$ |
| $\sqrt{v^2}_{halo}$ | $79.3$ to $261$ km/sec | $0.243$ km/sec |

The wimps values strongly disagree by several order of magnitude with the observations.

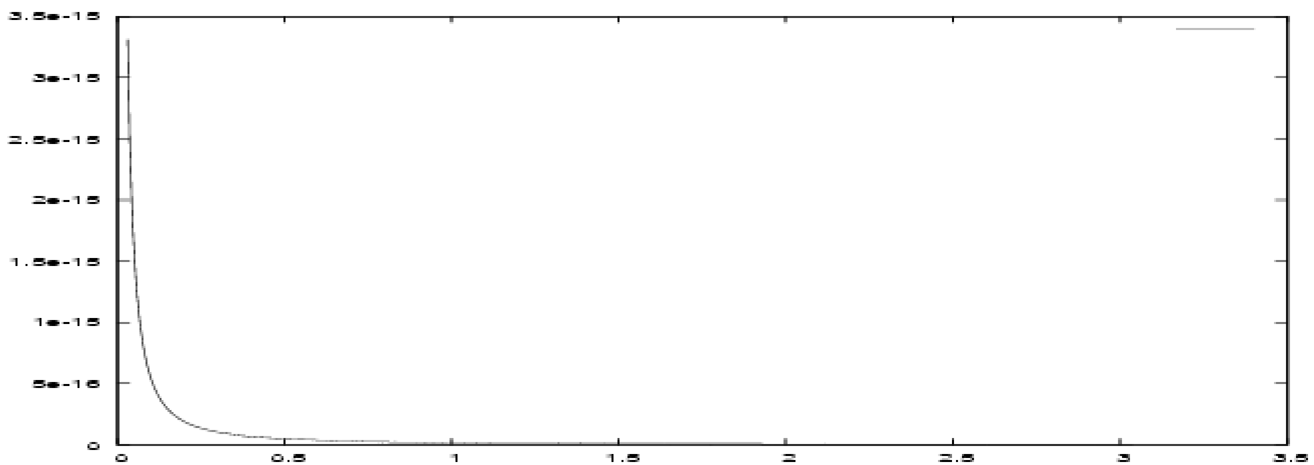


$\rho_{lin}(r)_{wimp}$ in $g/cm^3$ vs. $r$ in pc. Exhibits a cusp behaviour for $r \gtrsim 0.03$ pc.

# MASS OF THE DARK MATTER PARTICLE

**H. J. De Vega, N.G. Sanchez** ***Model independent analysis of dark matter points to a particle mass at the keV scale*** **Mon. Not. R. Astron. Soc. 404, 885 (2010)**

**D. Boyanovsky, H. J. de Vega, N.G. Sanchez** ***Constraints on dark matter particles from theory, galaxy observations and N-body simulations*** **Phys.Rev. D77 043518, (2008)**

# BOLTZMAN VLASOV EQUATION, TRANSFERT FUNCTION

**D. Boyanovsky, H. J. de Vega, N.G. Sanchez** ***The dark matter transfer function: free streaming, particle statistics and memory of gravitational clustering*** **Phys. Rev. D78: 063546, (2008)**

# DENSITY PROFILES, SURFACE DENSITY, DARK MATTER PARTICLE MASS

**H. J. de Vega, N.G. Sanchez** ***Gravity surface density and density profile of dark matter galaxies*** **IJMPA26:1057 (2011)**

**H. J. de Vega, P. Salucci, N.G. Sanchez** ***The mass of the dark matter particle from theory and observation*** **New Astronomy, 17, 653 -666 (2012)**

**Cosmological evolution of warm dark matter fluctuations I:**
**Efficient computational framework with Volterra integral equations**
**H.J. de Vega, N.G. Sanchez, Phys. Rev. D85, 043516 (2012)**

**Cosmological evolution of warm dark matter fluctuations II:**
**Solution from small to large scales and keV sterile neutrinos**
**H.J. de Vega, N.G. Sanchez, Phys. Rev. D85, 043517 (2012)**

## WARM DARK MATTER REPRODUCE

→**OBSERVED GALAXY DENSITIES AND VELOCITY DISPERSIONS**

→**SOLVES the OVERABUNDANCE ("satellite) PROBLEM**

**->OBSERVED SURFACE DENSITY VALUES OF DARK MATTER DOMINATED GALAXIES**

→**OBSERVED GALAXY CORED DENSITY PROFILES : QUANTUM MECHANICS**

# Galaxy Density Profiles: Cores vs. Cusps

Astronomical observations always find cored profiles for DM dominated galaxies. Selected references:

J. van Eymeren et al. A&A (2009), M. G. Walker, J. Peñarrubia, Ap J (2012). Reviews by de Blok (2010), Salucci & Frigerio Martins (2009).

Galaxy profiles in the linear regime: core size $\sim$ free streaming length (de Vega, Salucci, Sanchez, 2010)=

halo radius $r_0 = \begin{cases} 0.05 \text{ pc cusps for CDM (m > GeV).} \\ 50 \text{ kpc cores for WDM (m} \sim \text{keV).} \end{cases}$

N-body simulations for CDM give cusps (NFW profile).

N-body simulations for WDM :
quantum physics needed for fermionic DM !!!

CDM simulations give a precise value for the concentration $\equiv R_{virial}/r_0$. CDM concentrations disagree with observed

# Quantum Bounds on Fermionic Dark Matter

The Pauli principle gives the upper bound to the phase space distribution function of spin-$\frac{1}{2}$ particles of mass $m$:

$$f(\vec{r},\vec{p}) \leq 2$$

The DM mass density is given by:

$$\rho(\vec{r}) = m \int d^3p \, \frac{f(\vec{r},\vec{p})}{(2\,\pi\,\hbar)^3} = \frac{m^4}{2\,\hbar^3}\,\sigma^3(\vec{r})\,\bar{f}(\vec{r})\,K \ ,$$

where:

$\bar{f}(\vec{r})$ is the $\vec{p}-$average of $f(\vec{r},\vec{p})$ over a volume $m^3\,\sigma^3(\vec{r})$,

$\sigma(\vec{r})$ is the DM velocity dispersion, $\sigma^2(\vec{r}) \equiv < v^2(\vec{r}) > /3$

$K \sim 1$ a pure number.

The Pauli bound $\bar{f}(\vec{r}) \leq 2$ yields: $Q(\vec{r}) \equiv \frac{\rho(\vec{r})}{\sigma^3(\vec{r})} \leq K\,\frac{m^4}{\hbar^3}$

This is an absolute quantum upper bound on $Q(\vec{r})$ due to quantum physics, namely the Pauli principle.

$Q(\vec{r})$ can **never** take values larger than $K\,m^4/\hbar^3$.

In the classical limit $\hbar \to 0$ and the bound disappears.

# Classical physics breaks down near the galaxy center

$N$-body simulations point to cuspy phase-space densities

$Q(r) = Q_s \left(\frac{r}{r_s}\right)^{-\beta}$, $\beta \simeq 1.9 - 2$, $r_s =$ halo radius,

$Q_s =$ mean phase space density in the halo.

$Q(r)$ derived within classical physics tends to infinity for $r \to 0$ violating the Pauli principle bound.

Classical physics breaks down near the galaxy center.

For $\beta = 2$ the quantum upper bound on $Q(r)$ is valid for

$$r \geq r_q \equiv \frac{\hbar^{\frac{3}{2}}}{m^2} \sqrt{\frac{Q_s}{K}}\, r_s \; .$$

Observations yield: $30 < \frac{r_s}{\mathrm{pc}} < 5.10^4 \; , \; 2.10^{-5} < \frac{\hbar^{\frac{3}{2}} \sqrt{Q_s}}{(\mathrm{keV})^2} < 0.6$

The larger $Q_s$ and the smaller $r_s$ correspond to ultra compact dwarfs

The smaller $Q_s$ and the larger $r_s$ correspond to spirals.

# Dwarf galaxies as quantum objects

de Broglie wavelength of DM particles $\lambda_{dB} = \frac{\hbar}{m\,\sigma}$

$d =$ mean distance between particles,
$\sigma =$ DM mean velocity

$$d = \left(\frac{m}{\rho}\right)^{\frac{1}{3}} \quad , \quad Q = \rho/\sigma^3 \quad , \quad Q = \text{phase space density.}$$

ratio: $\mathcal{R} = \frac{\lambda_{dB}}{d} = \hbar \left(\frac{Q}{m^4}\right)^{\frac{1}{3}}$

Observed values: $2 \times 10^{-3} < \mathcal{R} \left(\frac{m}{\text{keV}}\right)^{\frac{1}{3}} < 1.4$

The larger $\mathcal{R}$ is for ultracompact dwarfs.
The smaller $\mathcal{R}$ is for big spirals.

$\mathcal{R}$ near unity (or above) means a QUANTUM OBJECT.

Observations alone show that compact dwarf galaxies are quantum objects (for WDM).

| Galaxy | $\frac{r_h}{\text{pc}}$ | $\frac{\sigma}{\frac{\text{km}}{\text{s}}}$ | $\frac{\hbar^{\frac{3}{2}}\ \sqrt{Q_h}}{(\text{keV})^2}$ | $\rho(0) / \frac{M_\odot}{(\text{pc})^3}$ | $\frac{M_h}{10^6\ M_\odot}$ |
|---|---|---|---|---|---|
| Willman 1 | 19 | 4 | 0.85 | 6.3 | 0.029 |
| Segue 1 | 48 | 4 | 1.3 | 2.5 | 1.93 |
| Leo IV | 400 | 3.3 | 0.2 | .19 | 200 |
| Canis Venatici II | 245 | 4.6 | 0.2 | 0.49 | 4.8 |
| Coma-Berenices | 123 | 4.6 | 0.42 | 2.09 | 0.14 |
| Leo II | 320 | 6.6 | 0.093 | 0.34 | 36.6 |
| Leo T | 170 | 7.8 | 0.12 | 0.79 | 12.9 |
| Hercules | 387 | 5.1 | 0.078 | 0.1 | 25.1 |
| Carina | 424 | 6.4 | 0.075 | 0.15 | 32.2 |
| Ursa Major I | 504 | 7.6 | 0.066 | 0.25 | 33.2 |
| Draco | 305 | 10.1 | 0.06 | 0.5 | 26.5 |
| Leo I | 518 | 9 | 0.048 | 0.22 | 96 |
| Sculptor | 480 | 9 | 0.05 | 0.25 | 78.8 |
| Boötes I | 362 | 9 | 0.058 | 0.38 | 43.2 |
| Canis Venatici I | 1220 | 7.6 | 0.037 | 0.08 | 344 |
| Sextans | 1290 | 7.1 | 0.021 | 0.02 | 116 |
| Ursa Minor | 750 | 11.5 | 0.028 | 0.16 | 193 |
| Fornax | 1730 | 10.7 | 0.016 | 0.053 | 1750 |
| NGC 185 | 450 | 31 | 0.033 | 4.09 | 975 |
| NGC 855 | 1063 | 58 | 0.01 | 2.64 | 8340 |
| Small Spiral | 5100 | 40.7 | 0.0018 | 0.029 | 6900 |
| NGC 4478 | 1890 | 147 | 0.003 | 3.7 | $6.55 \times 10^4$ |
| Medium Spiral | $1.9 \times 10^4$ | 76.2 | $3.7 \times 10^{-4}$ | 0.0076 | $1.01 \times 10^5$ |
| NGC 731 | 6160 | 163 | $9.27 \times 10^{-4}$ | 0.47 | $2.87 \times 10^5$ |
| NGC 3853 | 5220 | 198 | $8.8 \times 10^{-4}$ | 0.77 | $2.87 \times 10^5$ |
| NGC 499 | 7700 | 274 | $5.9 \times 10^{-4}$ | 0.91 | $1.09 \times 10^6$ |
| Large Spiral | $5.9 \times 10^4$ | 125 | $0.96 \times 10^{-4}$ | $2.3 \times 10^{-3}$ | $1. \times 10^6$ |

TABLE I: Observed values $r_h$, $\sigma$, $\sqrt{Q_h}$, $\rho(0)$ and $M_h$ covering from ultracompact objects and

# Quantum pressure vs. gravitational pressure

quantum pressure: $P_q$ = flux of momentum $= n\, v\, p$ ,

$v =$ mean velocity, momentum $= p \sim \hbar/\Delta x \sim \hbar\, n^{\frac{1}{3}}$ ,

particle number density $= n = \frac{M_q}{\frac{4}{3}\,\pi\, R_q^3\, m}$

galaxy mass $= M_q$ , galaxy halo radius $= R_q$

gravitational pressure: $P_G = \frac{G\, M_q^2}{R_q^2} \times \frac{1}{4\,\pi\, R_q^2}$

Equilibrium: $P_q = P_G \Longrightarrow$

$$R_q = \frac{3^{\frac{5}{3}}}{(4\,\pi)^{\frac{2}{3}}}\;\frac{\hbar^2}{G\, m^{\frac{8}{3}}\, M_q^{\frac{1}{3}}} = 10.6 \ldots \mathrm{pc}\left(\frac{10^6\, M_\odot}{M_q}\right)^{\frac{1}{3}}\;\left(\frac{\mathrm{keV}}{m}\right)^{\frac{8}{3}}$$

$$v = \left(\frac{4\,\pi}{81}\right)^{\frac{1}{3}}\;\frac{G}{\hbar}\; m^{\frac{4}{3}}\; M_q^{\frac{2}{3}} = 11.6\,\frac{\mathrm{km}}{\mathrm{s}}\;\left(\frac{\mathrm{keV}}{m}\right)^{\frac{4}{3}}\;\left(\frac{M_q}{10^6\, M_\odot}\right)^{\frac{2}{3}}$$

for WDM the values of $M_q,\ R_q$ and $v$ are consistent with the dwarf galaxy observations !! .

Dwarf spheroidal galaxies can be supported by the fermionic quantum pressure of WDM.

## In the presence of angular momentum $L$

Adds the centrifugal pressure: $P_L = \frac{L^2}{M\ R^3}\ \frac{1}{4\,\pi\,R^2}$

Equilibrium: $P_q + P_L = P_G$:

$$\left(\frac{3}{4\,\pi}\right)^{5/3}\ \frac{\hbar^2\ M^{5/3}}{m^{8/3}\ R^5} + \frac{L^2}{4\,\pi\ M\ R^5} = \frac{G\ M^2}{4\,\pi\ R^4}$$

$$\Rightarrow \quad R = \frac{L^2}{G\ M^3} + \frac{3^{5/3}}{(4\,\pi)^{2/3}}\ \frac{\hbar^2}{G\ m^{8/3}\ M^{1/3}}\ .$$

We estimate $L^2$ as $L^2 \sim \frac{1}{2}\ M^2\ R^2\ 3\ \sigma^2$.

The $\frac{1}{2}$ factor comes from averaging the $\sin^2$ of the an

between the momentum $\vec{p}$ and the particle position $\vec{r}$

$$R = 10.6\text{pc}\left(\frac{10^6\ M_\odot}{M}\right)^{\frac{1}{3}}\ \left(\frac{\text{keV}}{m}\right)^{\frac{8}{3}} + 3.48\text{pc}\ \frac{10^6\ M_\odot}{M}\ \left(\frac{\sigma}{10\ \frac{\text{km}}{\text{s}}}\right.$$

The angular momentum increases the size $R$.

For dwarf galaxies, $R$ and $\sigma$ have the same order of

magnitude for $L > 0$ and for $L = 0$.

## The quantum radius $r_q$ for different kinds of DM

| DM type | DM particle mass | $r_q$ | |
|---|---|---|---|
| CDM | $1 - 100$ GeV | $1 - 10^4$ meters | in practice zero |
| WDM | $1 - 10$ keV | $0.1 - 1$ pc | compatible with observed cores |
| HDM | $1 - 10$ eV | kpc - Mpc | too big ! |

# Self-gravitating Fermions in the Thomas-Fermi approach

WDM is non-relativistic in the MD era. A single DM halo in late stages of formation relaxes to a time-independent form especially in the interior.

Chemical potential: $\mu(r) = \mu_0 - m\,\phi(r)$ , $\phi(r) =$ grav. pot.

Poisson's equation: $\frac{d^2\mu}{dr^2} + \frac{2}{r}\,\frac{d\mu}{dr} = -4\,\pi\,G\,m\,\rho(r)$

$\rho(0) =$ finite for fermions $\Longrightarrow \frac{d\mu}{dr}(0) = 0$.

Density $\rho(r)$ and pressure $P(r)$ in terms of the distribution function $f(E)$:

$\rho(r) = \frac{m}{\pi^2\,\hbar^3}\int_0^\infty p^2\,dp\,f[\frac{p^2}{2\,m} - \mu(r)]$

$P(r) = \frac{m}{3\,\pi^2\,\hbar^3}\int_0^\infty p^4\,dp\,f[\frac{p^2}{2\,m} - \mu(r)]$

Boundary condition at

$r = R = R_{200} \sim R_{vir}$ , $\rho(R_{200}) \simeq 200\,\bar{\rho}_{DM}$

# Thomas-Fermi approximation: solutions

$$M(R) = \frac{(3\,\pi)^2\,\hbar^6}{256\,G^3\,m^8\,R^3}\;\;\xi_0^5\;\;|\nu'(\xi_0)|$$

$$P(r) = \frac{\pi^{\frac{4}{3}}}{3}\;\hbar^2\;\left[\frac{\rho(0)}{\beta(\xi_0)\;m^4}\right]^{\frac{5}{3}}\;\int_0^\infty y^4\,dy\;\Psi\left(y^2-\nu(\xi)\right)$$

$L_0$ and $M(R)$ turn to be of the order of the Jeans' length and the Jeans' mass, respectively.

The chemical potential at $r = 0$ fixed by the value of $Q(0)$.

Using observed values of $Q(0)$, we obtain halo radius $r_s \sim 0.1 - 10$ kpc, galaxy masses $10^5 - 10^7\;M_\odot$ and velocity dispersions, all consistent with the observations of dwarf galaxies.

The Thomas-Fermi approach gives realistic halo radii, larger than the quantum lower bound $r_q$, as expected.

Fermionic WDM treated quantum mechanically is able to reproduce the observed DM cores of galaxies.

# Self-gravitating Fermions in the Thomas-Fermi approach

The Thomas-Fermi approach gives physical galaxy magnitudes: mass, halo radius, phase-space density and velocity dispersion fully compatible with observations from the largest spiral galaxies till the ultracompact dwarf galaxies for a WDM particle mass around 2 keV.

Compact dwarf galaxies are close to a degenerate WDM Fermi gas while large galaxies are classical WDM Boltzmann gases.

Fermionic WDM treated quantum mechanically is able to reproduce the observed galaxies.

C. Destri, H. J. de Vega, N. G. Sanchez, arXiv:1204.3090 to appear in New Astronomy. ‘Quantum WDM fermions and gravitation determine the observed galaxy structures’, arXiv:1301.1864.

we derive the local equation of state:

$$P(r) = \frac{1}{3}\, v^2(r)\, \rho(r) \quad .$$

) the hydrostatic equilibrium equation

$$\frac{dP}{dr} + \rho(r)\, \frac{d\phi}{dr} = 0 \, .$$

ion of state generalizes the local perfect fluid equation of state for $r$-dependent velocity $v(r)$.
e perfect fluid equation of state is recovered both in the classical dilute limit and in the quan

$P(r)$ between eqs.(2.6) and (2.7) and integrating on $r$ gives

$$\frac{\rho(r)}{\rho(0)} = \frac{v^2(0)}{v^2(r)}\, e^{-3 \int_0^r \frac{dr'}{v^2(r')}\, \frac{d\phi}{dr'}} \quad .$$

) this relation reduces to the baryotropic equation. Inserting this expression for $\rho(r)$ in the Poiss

$$\frac{d^2\phi}{dr^2} + \frac{2}{r}\, \frac{d\phi}{dr} = 4\,\pi\, G\, m\, \rho(0)\, \frac{v^2(0)}{v^2(r)}\, e^{-3 \int_0^r \frac{dr'}{v^2(r')}\, \frac{d\phi}{dr'}} \quad .$$

quation generalizes the corresponding equation in the self-gravitating Boltzmann gas when $v^2($

# RESULTS

## All the obtained density profiles are cored.

**The Core Sizes are in agreement with the observations**

**from the compact galaxies where $r_h$ ~ 20 pc till the spiral and elliptical galaxies where $r_h$ ~ 0.2 - 60 kpc.**

**The larger and positive is the chemical potential $\nu(0)$, the smaller is the core. The minimal one arises in the degenerate case $\nu(0)$ --> to +infinity (compact dwarf galaxies).**

**And**

**The Phase-space Density**

**The Galaxy halo Masses.**

**Agreement is found in all the range of galaxies for a DM particle mass m around 2 keV.**

**Error bars of the observational data are not shown but they are at least about 10-20 %.**

# Galaxy data vs. Thomas-Fermi

Mass, halo radius, velocity dispersion and central density from a broad variety of galaxies: ultracompact galaxies to giant spirals, Willman 1, Segue 1, Canis Venatici II, Coma-Berenices, Leo II, Leo T, Hercules, Carina, Ursa Major I, Draco, Leo I, Sculptor, Boötes, Canis Venatici I, Sextans, Ursa Minor, Fornax, NGC 185, NGC 855, NGC 4478, NGC 731, NGC 3853, NGC 499 and a large number of spiral galaxies.

Phase-Space distribution function $f(E/E_0)$: Fermi-Dirac ($F(x) = \frac{1}{e^x+1}$) and out of equilibrium sterile neutrinos give similar results.

$E_0 =$ effective galaxy temperature (energy scale).

$E_0$ turns to be $10^{-3}$ $^o$K $< E_0 <$ 50 $^o$K

colder = ultracompact, warmer = large spirals.

$E_0 \sim m \; < v^2 >_{\rm observed}$ for $m \sim 2$ keV.

# $Q$ vs. halo radius. Galaxy observations vs. Thomas-Fermi

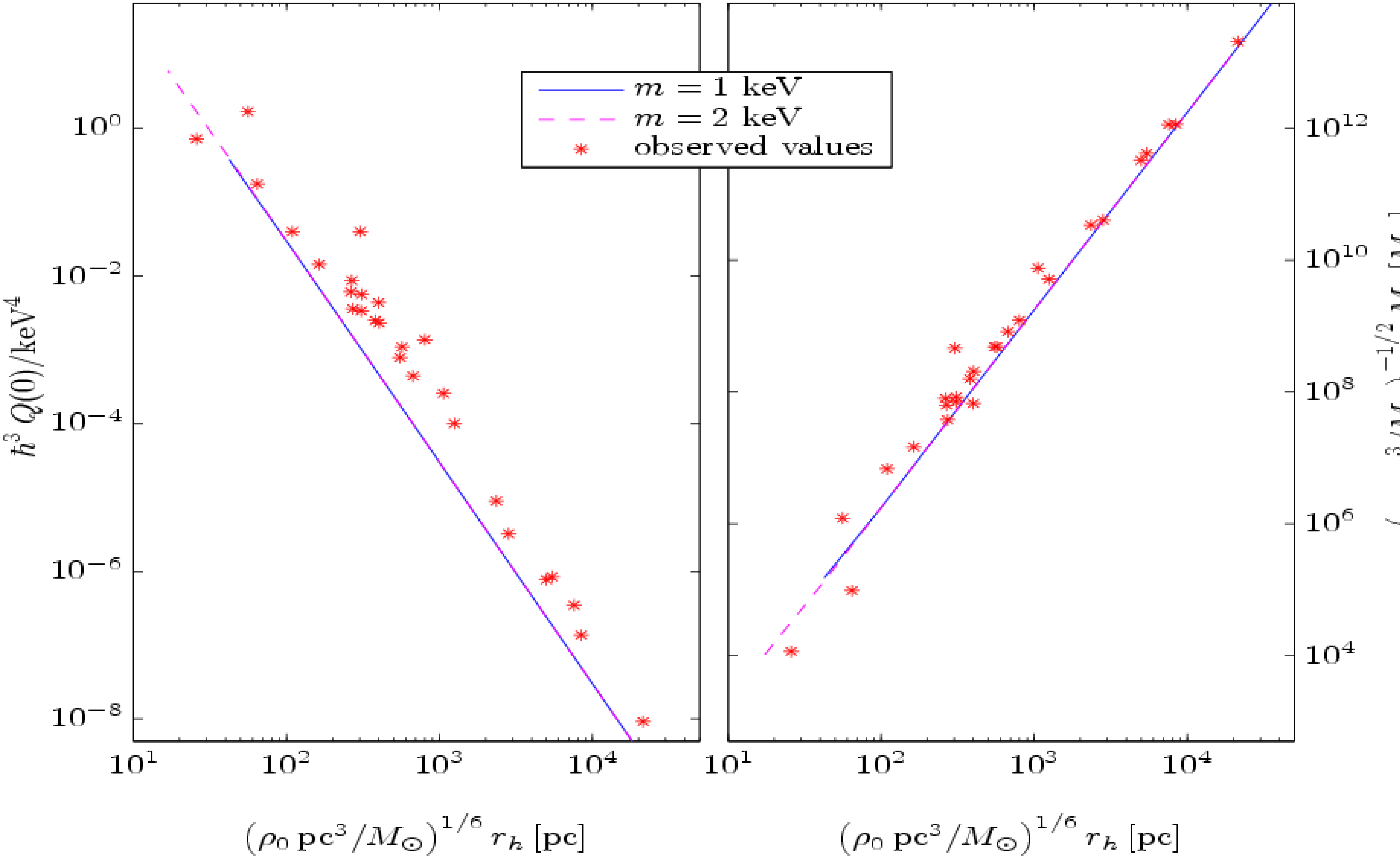


observed $Q = \rho/\sigma^3$ from stars are upper bounds for DM $Q$

# Density and velocity profiles from Thomas-Fermi

**Cored** density profile and velocity profile obtained from Thomas-Fermi.

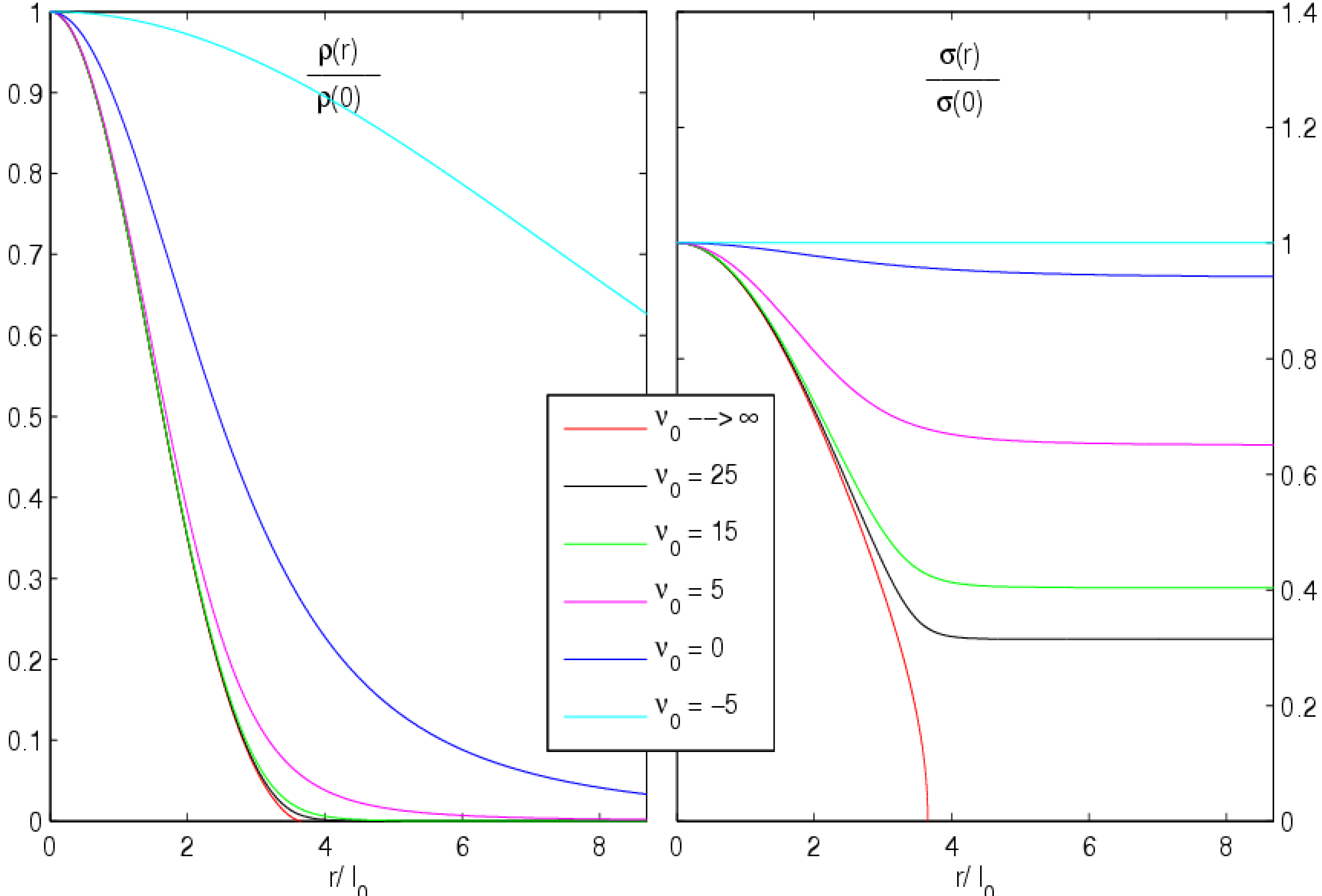

| Galaxy | $\frac{r_h}{\text{pc}}$ | $\frac{\sigma}{\frac{\text{km}}{\text{s}}}$ | $\frac{\hbar^{\frac{3}{2}}\sqrt{Q_h}}{(\text{keV})^2}$ | $\rho(0)/\frac{M_\odot}{(\text{pc})^3}$ | $\frac{M_h}{10^6\ M_\odot}$ |
|---|---|---|---|---|---|
| Willman 1 | 19 | 4 | 0.85 | 6.3 | 0.029 |
| Segue 1 | 48 | 4 | 1.3 | 2.5 | 1.93 |
| Leo IV | 400 | 3.3 | 0.2 | .19 | 200 |
| Canis Venatici II | 245 | 4.6 | 0.2 | 0.49 | 4.8 |
| Coma-Berenices | 123 | 4.6 | 0.42 | 2.09 | 0.14 |
| Leo II | 320 | 6.6 | 0.093 | 0.34 | 36.6 |
| Leo T | 170 | 7.8 | 0.12 | 0.79 | 12.9 |
| Hercules | 387 | 5.1 | 0.078 | 0.1 | 25.1 |
| Carina | 424 | 6.4 | 0.075 | 0.15 | 32.2 |
| Ursa Major I | 504 | 7.6 | 0.066 | 0.25 | 33.2 |
| Draco | 305 | 10.1 | 0.06 | 0.5 | 26.5 |
| Leo I | 518 | 9 | 0.048 | 0.22 | 96 |
| Sculptor | 480 | 9 | 0.05 | 0.25 | 78.8 |
| Boötes I | 362 | 9 | 0.058 | 0.38 | 43.2 |
| Canis Venatici I | 1220 | 7.6 | 0.037 | 0.08 | 344 |
| Sextans | 1290 | 7.1 | 0.021 | 0.02 | 116 |
| Ursa Minor | 750 | 11.5 | 0.028 | 0.16 | 193 |
| Fornax | 1730 | 10.7 | 0.016 | 0.053 | 1750 |
| NGC 185 | 450 | 31 | 0.033 | 4.09 | 975 |
| NGC 855 | 1063 | 58 | 0.01 | 2.64 | 8340 |
| Small Spiral | 5100 | 40.7 | 0.0018 | 0.029 | 6900 |
| NGC 4478 | 1890 | 147 | 0.003 | 3.7 | $6.55 \times 10^4$ |
| Medium Spiral | $1.9 \times 10^4$ | 76.2 | $3.7 \times 10^{-4}$ | 0.0076 | $1.01 \times 10^5$ |
| NGC 731 | 6160 | 163 | $9.27 \times 10^{-4}$ | 0.47 | $2.87 \times 10^5$ |
| NGC 3853 | 5220 | 198 | $8.8 \times 10^{-4}$ | 0.77 | $2.87 \times 10^5$ |
| NGC 499 | 7700 | 274 | $5.9 \times 10^{-4}$ | 0.91 | $1.09 \times 10^6$ |
| Large Spiral | $5.9 \times 10^4$ | 125 | $0.96 \times 10^{-4}$ | $2.3 \times 10^{-3}$ | $1. \times 10^6$ |

TABLE I: Observed values $r_h$, $\sigma$, $\sqrt{Q_h}$, $\rho(0)$ and $M_h$ covering from ultracompact objects and

# THE MINIMAL GALAXY MASS

**A minimal galaxy mass and minimal velocity dispersion are found.**

**This in turn implies a minimal mass m_min =1.91 keV for the WDM particle.**

**This minimal WDM mass is a universal value, independent of the WDM particle physics model because only relies on the degenerate quantum fermion state, which is universal whatever is the non-degenerate regime.**

**These results and the observed halo radius and mass of the compact galaxies also provide further indication that the WDM particle mass m is approximately around 2 keV.**

**More precise data will make this estimation more precise.**

# Minimal galaxy mass from degenerate WDM

The halo radius, the velocity dispersion and the galaxy mass take their minimum values for degenerate WDM:

$$r_{h\ min} = 24.51\ldots \ \mathrm{pc} \ \left(\frac{m}{\mathrm{keV}}\right)^{\frac{4}{3}} \ \left[\rho(0) \ \frac{\mathrm{pc}^3}{M_\odot}\right]^{\frac{1}{6}}$$

$$M_{min} = 2.939\ldots \ 10^5 \ M_\odot \ \left(\frac{\mathrm{keV}}{m}\right)^4 \ \sqrt{\rho(0) \ \frac{\mathrm{pc}^3}{M_\odot}}$$

$$\sigma_{min}(0) = 2.751\ldots \ \frac{\mathrm{km}}{\mathrm{s}} \ \left(\frac{\mathrm{keV}}{m}\right)^{\frac{4}{3}} \ \left[\rho(0) \ \frac{\mathrm{pc}^3}{M_\odot}\right]^{\frac{1}{3}} \ .$$

These minimum values correspond to the observations of compact dwarf galaxies.

Lightest known compact dwarf galaxy is Willman I:
$M_{Willman\ I} = 2.9 \ 10^4 \ M_\odot$

Imposing $M_{Willman\ I} > M_{min}$ yields the lower bound for the WDM particle mass: $m > 1.91$ keV.

## WARM DARK MATTER REPRODUCE

**→OBSERVED GALAXY DENSITIES AND VELOCITY DISPERSIONS**

**→OBSERVED GALAXY CORED DENSITY PROFILES**

**->OBSERVED SURFACE DENSITY VALUES OF DARK MATTER DOMINATED GALAXIES**

**→SOLVES the OVERABUNDANCE (“satellite) PROBLEM and the CUSPS vs CORES Problem**

## • WDM OVERALL CONCLUSION

- **To conclude, we find it is highly remarkable that in the context of warm dark matter, the quantum description provided by this semiclassical framework, (quantum WDM and classical gravitation), is able to reproduce such broad variety of galaxies.**

- **The resulting galaxy, halo radius, galaxy masses and velocity dispersion are fully consistent with observations for all different types of galaxies. Fermionic WDM treated quantum mechanically, as it must be, is able to reproduce the observed galactic cores and their sizes. In addition, WDM simulations produce the right DM structures in agreement with observations for scales > kpc.**

# WDM + BARYONS

**Baryons have not been included in this study. This is fully justified because on one hand dwarf compact galaxies are composed today 99.99 % of DM, and** on the other hand **the baryon fraction in large galaxies can reach values up to 1 - 3 %.**

**Since Fermionic WDM by itself produces galaxies and structures in agreement with observations for all types of galaxies, masses and sizes, the effect of including baryons is expected to be a small correction to these pure WDM results, consistent with the fact that dark matter is in average six times more abundant than baryons.**

## Summary and Conclusions

- Combining theoretical evolution of fluctuations through the Boltzmann-Vlasov equation with galaxy data points to a DM particle mass 3 - 10 keV. $T_d$ turns to be model dependent. The keV mass scale holds independently of the DM particle physics model.

- Universal Surface density in DM galaxies $[\mu_{0D} \simeq (18 \text{ MeV})^3]$ explained by keV mass scale DM. Density profile scales and decreases for intermediate scales with the spectral index $n_s$ : $\rho(r) \sim r^{-1-n_s/2}$ and $\rho(r) \sim r^{-2}$ for $r \gg r_0$.

H. J. de Vega, P. Salucci, N. G. Sanchez, 'The mass of the dark matter particle from theory and observations', New Astronomy, 17, 653 (2012).

H. J. de Vega, N. Sanchez, 'Model independent analysis of dark matter points to a particle mass at the keV scale',

**END**

**THANK YOU FOR YOUR ATTENTION**

## IN PROGRESS

**H. J. de Vega, N. G. Sanchez:**

**BLACK HOLES FORMED by WDM and BARYONS**

**(GALACTIC SUPERMASSIVE, STELLAR)**

**------------------**

**Galaxy Structure from Classical Cosmological Boltzmann-Vlasov equations: Generalized Larson equations**

**And other results…..**

# École Internationale Daniel Chalonge

*22 Years of Activity* — *Calling for Understanding*

**SCIENCE WITH GREAT INTELLECTUAL ENDEAVOUR AND A HUMAN FACE**
**LA SCIENCE QUI DONNE ENVIE : UNE GRANDE AVENTURE SCIENTIFIQUE ET HUMAINE**

# PROGRAMME 2013

**15 MARCH 2013** : **"Présentation du Programme 2013 et des Dernières Nouvelles Scientifiques de l'Univers »** Bâtiment Perrault, Observatoire de Paris

**4-7 APRIL 2013** : **"Latest News from the Universe, Dark Matter Galaxies and Particle Physics"** Palazzo de l'Università & Palazzo Graneri, Piamonte Région, Turin, Italy

**16 MAY 2013** : **Spring Open Session of Scientific Culture 2013 Session Ouverte de Printemps de Culture Scientifique 2013 : "L'Homme et l'Univers"** Bâtiment Perrault, Observatoire de Paris, Paris

**30 MAY 2013** : **Rencontre de Culture Scientifique "Voyage à travers l'Univers : De ses Origines à nos Jours"** Cité Internationale Universitaire de Paris, Paris

**4-7 JUNE 2013** : **Chalonge Meudon Workshop 2013 "Warm Dark Matter Galaxies in Agreement with Observations : Formation, Evolution and Supermassive Black Holes"** Observatoire de Paris, Château de Meudon-CIAS, Meudon

**23-26 JULY 2013** : **The 17th Paris Cosmology Colloquium Chalonge 2013: "The New Standard Model of the Universe: ΛWDM – Warm Dark Matter: "Theory and Observations"** Bâtiment Perrault, Observatoire de Paris, Paris

**26 JULY 2013** : **Summer Open Session of Scientific Culture 2013 / Session Ouverte d'Eté de Culture Scientifique 2013 : A Surprise Session**

**AUTOMME 2013** : **Cycle Les grandes questions posées aujourd'hui à la Science : 1ère Question : Où va la Science ?** Cité Internationale Universitaire de Paris, Paris

**And Other Events...**

N. G. SANCHEZ * H. J. DE VEGA * M. C. FALVELLA * A. ZANINI * M. RAMON MEDRANO * A. PERISSA and other colleagues
http://chalonge.obspm.fr

l'Observatoire de Paris · LERMA · UPMC · CNRS · MAIRIE DE PARIS · ACAV · îledeFrance